

Nanostructured Coatings with Advanced  
Antimicrobial Properties

by

Charis Isobel Winder

A thesis submitted in partial fulfilment for the requirements for the degree of  
MSc by Research at the University of Central Lancashire

May 2019





## STUDENT DECLARATION FORM

Type of Award                      Masters by Research

School                                      School of Physical Science and computing

Concurrent registration for two or more academic awards

I declare that while registered as a candidate for the research degree, I have not been a registered candidate or enrolled student for another award of the University or other academic or professional institution

---

Material submitted for another award

I declare that no material contained in the thesis has been used in any other submission for an academic award and is solely my own work

---

Signature of Candidate            Charis Winder

Type of Award                      MSc by Research

School                                      School of Physical Science and Computing

## List of Contents

Acknowledgments .....	vii
List of tables .....	viii
List of figures .....	viii-ix
List of equations .....	ix
Abbreviations.....	x-xi
Abstract .....	xii
1. Introduction .....	1
1.1 Antimicrobial surface coatings .....	1
1.2 Methods for generating surface coatings .....	5
1.2.1 Layer-by-Layer Approach .....	5
1.2.2 Other approaches for generating surface coatings .....	7
1.3 Materials with antimicrobial activity .....	8
1.3.1 The use of nanoparticles for antimicrobial surface coatings ...	9
1.3.2 Uses of polymer surfaces .....	11
1.4 Antimicrobial agents used in this study .....	13
1.4.1 Chitosan .....	13
1.4.2 Lysozyme .....	14
1.4.3 Nafion .....	16
1.4.4 Polyvinylpyrrolidone .....	17
1.4.5 QPDMAEMA – PLMA .....	18
1.5 Gram-positive and Gram-negative bacteria .....	18
2. Materials and Methodology .....	20
2.1 Materials .....	20

2.2	Methods.....	20
2.3	Quartz crystal Microbalance with dissipation monitoring .....	21
2.4	Antimicrobial testing .....	23
2.5	FT-IR .....	25
2.6	Atomic Force microscopy .....	25
2.7	Contact Angle Analysis .....	26
2.8	UV-Vis and Transparency analysis .....	29
3.	Results and Discussion .....	30
3.1	Coatings formed using Lysozyme and Chitosan .....	30
3.1.1	FT-IR .....	30
3.1.2	QCM-D .....	34
3.1.3	Antimicrobial testing .....	38
3.1.4	AFM .....	41
3.1.5	Contact Angle analysis .....	44
3.1.6	UV-Vis analysis .....	46
3.2	Coatings formed using QPDAEMA – PLMA .....	49
3.2.1	QCM-D .....	49
3.2.2	Antimicrobial testing .....	50
3.3	Coatings formed using Polyvinylpyrrolidone .....	51
3.3.1	FT-IR .....	51
3.3.2	QCM-D .....	53
3.3.3	Antimicrobial testing .....	56
3.3.4	Contact Angle Analysis .....	58
4.	Summary .....	59
5.	Conclusion .....	60
	References .....	61



## Acknowledgements

I would like to thank my supervisor Dr Antonios Kelarkais for his continuous support, guidance and expertise throughout this project. I would also like to thank my second supervisor Harry Eccles for his time and support for which I am grateful.

Thank you also to the Uclan science technicians for all there help throughout the course of this project.

Thank you also to Ella Gibbons for all her assistance with the antimicrobial testing and thank you to Kira Heslop for lending a helping hand when needed.

A massive thanks to my Mum Karen, Dad Tim and Grandma June, who's constant support love and encouragement has enabled me to complete this year.

I would also like to say a massive thank you to Bryony Board who's support this year, as always has been invaluable, especially within the last month of this project for which I will always be gratefully.

I would also like to say thank you to Hannah Lawrence for always being on hand for last minute proof reading.

Thank you too Zack Anderson, Matt Davies and Joe Rawlinson, Jackie Wong for always being on hand to help with both Chemistry and IT knowledge, as well as always being there to put a smile on my face whenever things weren't going to plan.

Finally I would like to say a special thank you to Mark Sullivan for proof reading through my final drafts, helping me to correct any errors and for all round moral support.

## List of Tables

Table 1 .....	45
Table 2 .....	59

## List of Figure

Figure 1 .....	3
Figure 2 .....	6
Figure 3 .....	14
Figure 4 .....	15
Figure 5 .....	16
Figure 6 .....	17
Figure 7.....	18
Figure 8.....	25
Figure 9 .....	27
Figure 10 .....	29
Figure 11 .....	32
Figure 12 .....	34
Figure 13 .....	36
Figure 14 .....	38
Figure 15 .....	39
Figure 16 .....	40



Figure 17 .....	41
Figure 18 .....	42
Figure 19 .....	43
Figure 20 .....	43
Figure 21 .....	44
Figure 22 .....	44
Figure 23 .....	48
Figure 24 .....	49
Figure 25 .....	50
Figure 26 .....	51
Figure 27 .....	53
Figure 28 .....	55
Figure 29 .....	56
Figure 30 .....	57
Figure 31 .....	57
Figure 32 .....	58

#### List of equations

Equation 1 .....	23
Equation 2 .....	23
Equation 3 .....	23
Equation 4 .....	30

## Abbreviations

(N/L)x6	Nafion and Lysozyme Bilayer with 6 layers of each
(N/C)x6	Nafion and Chitosan Bilayer with 6 layers of each
(N/M)x3	Nafion and QPDMAEMA – PLMA Diblock with 3 layers of each
(N/P)x3	Nafion and Polyvinylpyrrolidone with 3 layers of each
(N/L/N/C)x2	Nafion, Lysozyme and Chitosan with 2 layers of Chitosan, 2 layers of Lysozyme with 4 layers Nafion between each
(N/P/N/L)x1	Nafion, Polyvinylpyrrolidone Lysozyme with 1 layer of Polyvinylpyrrolidone, 1 layer of Lysozyme with 2 layers of Nafion between each
(N/P/N/C)x1	Nafion, Polyvinylpyrrolidone Chitosan with 1 layer of Polyvinylpyrrolidone, 1 layer of chitosan and 2 layers of Nafion between each
CFU	Colony forming units

QCM-D	Quartz Crystal Microbalance with Dissipation Monitoring
FT-IR	Fourier Transformed Infrared Spectroscopy
AFM	Atomic Force Microscopy
UV-Vis	Ultra Violet Visible Spectroscopy
E.coli	Escherichia Coli
S.aureus	Staphylococcus Aureus
PVP	Polyvinylpyrrolidone
QPDMAEMA – PLMA	Quaternarized poly(2-Dimethylaminoethyl Methacrylate) Lauryl methacrylate

## Abstract

Antimicrobial surface coatings are important for the prevention of bacteria growth, having extensive applications in areas such as food packaging and medical applications. In this study ionomer Nafion (N) was used, in conjunction with synthetic polymer (QPDMAEA-PLMA Diblock (M) and Polyvinylpyrrolidone (P)) and naturally occurring biocides (Lysozyme (L) and Chitosan (C)), to synthesise antimicrobial surface coatings. This was achieved through a layer-by-layer assembly method, using a Quartz Crystal Microbalance with Dissipation Monitoring (QCM-D). Nafion (negatively charged) was deposited in alternating layers with the positively charged materials, this allowed electrostatic bonds to form between each of the layers, allowing for a durable and stable coating. Electrostatic forces and hydrogen bonding were observed through FT-IR analysis showing the interactions between the positive and negatively charged layers. The coatings were tested for antimicrobial effectiveness, with all coatings showing antimicrobial properties and (N/L/N/C)x2 and (N/Lx6) showing more than 99.9% reduction in bacteria.

Atomic Force Microscopy (AFM) was used to analyse the coatings (N/L/N/C)x2, (N/L)x6 and (N/C)x6, these all showed high levels of surface roughness. Contact Angle measurements was used to analyse the coatings hydrophobicity. Coatings (N/L)x6, (N/C)x6, (N/L/N/C)x2, (N/P)x3, and (N/P/N/L)x1 all showed wettability values between 75°-45°. UV-Vis spectroscopy was used to test the coatings transparency with (N/L)x6, (N/C)x6 and (N/L/N/C)x2 showing transparency.

# Chapter One

## Introduction

Harmful microbes are responsible for the spread of a variety of diseases, some of which might become lethal. Not only do these microbes have a negative impact on human health but also on the global economy taking into account the substantial expenses related to preventive and curative measures<sup>1</sup>. There are many different methods that can be used to prevent or hinder the activity of these harmful microbes. One of the most common ways is the use of antibiotics, however due to the increasing problem of antibiotic resistance, this approach by itself is not sufficient in the long run. Other strategies rely on antimicrobial coatings to prevent microbes growing and spreading from a given surface. However, despite significant research efforts in this field there are several persisting challenges related to their toxicity, environmental impact, their structural stability, particularly under harsh conditions, durability and preparation cost.

### 1.1 Antimicrobial Surface Coatings

Antimicrobial surface coatings can be applied to surfaces to help to reduce and prevent the spread of bacteria and harmful microorganisms both on and from the surface. Antibacterial surfaces usually work either by a bactericidal action or an anti-adhesion action in which the bacteria is stopped from adhering to the surface<sup>2</sup>. Biofilms are the growth of a collection of one or more microorganisms that adhere to a surface and grow there<sup>3</sup>. This occurs when microorganisms settle onto a surface and form a colonies, which develop the formation of the biofilm. This biofilm is an ideal environment for bacteria to growth<sup>4</sup> and includes

examples such as dental plaque and algae<sup>5</sup>. Biofilm formation can adhere to numerous different surfaces; including healthcare instruments, food processing equipment, mass transportation vehicles, door handles, shared computers, etc. Biofilms account for a number of different infections that invade the body and impose serious threats to human health, as well as having a negative impact economically due to the cost of their removal and prevention. One way to interfere with this process is to use antibiotics to remove these microbes from the surface<sup>5</sup>. Unfortunately, excessive use of antibiotics leads to enhanced antibiotic resistivity<sup>6</sup>, necessitating the development of alternative pathways to tackle this major challenge.

, Antimicrobial surface coatings show great promise in preventing the growth of harmful microbes. Where antimicrobial properties can be affected by numerous factors including; molecular weight, hydrophobicity and hydrophilicity, of the coatings<sup>4</sup>.

A number of other approaches have been systematically explored as shown in Figure 1. Those strategies include; the surface immobilization of antimicrobials, surface coatings that release antimicrobials into their surroundings, antimicrobials that are tethered to the surface, and antimicrobials that are contained within a matrix or hydrogel upon the surface<sup>7</sup>.

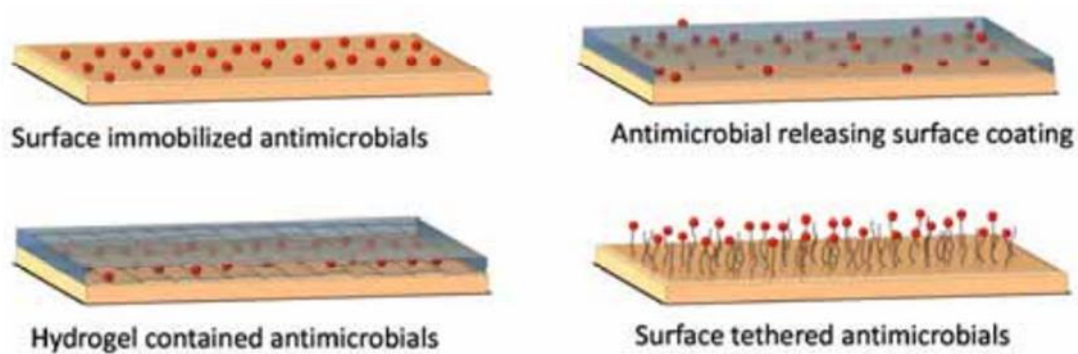


Figure 1. Schematic representation of four different types of antimicrobial surface coatings<sup>7</sup>.

There are several types of surface coatings that can be used for antimicrobial action (Figure 1). One of the coating that can be used, as shown above in Figure 1, is surface immobilized antimicrobials. In these type of coatings, the antimicrobial substance is immobilized on the surface of the coating enabling it to act upon bacteria by contact killing. Contact killing layer-by-layer assemblies have an advantage over coatings which release bactericidal agents, as a lower amount of biological agents are released into the environment, meaning that their impact on the surrounding environment is much lower than release surfaces<sup>2</sup>. Another advantage of coatings which act through contact killing is that they tend to have a longer life span compared with release based coatings. This is mainly due to their greater stability as a result of being immobilised to the surface<sup>2</sup> It is possible to adjust the stability of a contact killing substance within the coating, meaning there are possibilities for the substance not only to kill any attached bacteria, but also allowing the substance to be released into the surrounding area, by reducing the stability, enabling it to killing bacteria in a surrounding area as a result<sup>2</sup>.

Coatings can also act on bacteria by releasing a compound that is capable of killing bacteria<sup>4</sup>. A number of surface coating approaches have been developed to give a controlled release of an active antimicrobial component over time. The release profile of the coatings should be accurately controlled to avoid excessive material that could contribute towards antimicrobial resistance. At the same time, the released concentration should exceed a minimal value so that it does not lead to sub-inhibitory release. One powerful tool to control the release of the active ingredient is the use of multi-layer coatings comprising degradable polymers that are decomposed slowly over time<sup>7</sup>.

It is also possible to use hydrogels to form antimicrobial surface coatings. Hydrogels are highly hydrated biomaterials which can be produced from both natural and synthetic polymers. Hydrogels are able to act as a starting platform for developing antimicrobials as the antimicrobial agent can be encapsulated and immobilized onto the hydrogel. Some of the materials well suited to forming antimicrobial hydrogels are chitosan, alginate and dextran. Due to hydrogel biocompatibility they have been able to be designed to have properties similar to natural tissue, which have enabled them to be developed for applications in wound healing and surface coatings for implants<sup>8</sup>.

Surface tethered antimicrobials are another type of surface coating used for antimicrobial application. In immobilised surface coatings the antimicrobial in the surface coating is limited to acting on the bacteria by contact killing due to their lack of mobility. In tethered surface coatings however, the antimicrobials are more mobile to move and interact with bacteria around the surface. Tethered antimicrobials are therefore free to attack bacteria in a similar way to release peptides, without the bacteria making contact with the surface or the antimicrobial actually being released from the surface. These mean that they are capable of



potentially affecting a broader spectrum of bacteria than immobilised surface coatings<sup>9</sup>.

Halogen-based antibacterial agents, derived from nitrogen, *N*-halamines are becoming popular in the use as disinfectants and can either be described as reactive or non-reactive<sup>10</sup>. Reactive *N*-halamines are compounds that contain tethering groups. These groups are capable of forming covalent bonds with the surface<sup>11</sup>, meaning these types of coatings can show prolonged stability. The non-reactive *N*-halamines can be divided into two groups: non-polymeric and polymeric. The non-polymeric reactive *N*-halamines are composed of two main groups: the biocide group and the tethering group. The tethering groups include siloxane and epoxide. When the coatings are applied to surfaces, ideally they should have an attractive look and be warm to touch as well as being durable and resist corrosion. This is especially important for surface coatings being used to coat surfaces that are in regular use by the public. Alongside this, they still need to possess antibacterial properties to prevent the growth and spread of bacteria to and from that surface. Over the past several years surface coatings have been developed for many different applications, such as solar panels<sup>12</sup>, biomaterials to stimulate tissue growth on implants, etc<sup>13</sup>.

## 1.2 Methods for Generating Surface Coatings

### 1.2.1 Layer-by-Layer Approach

Stable surface coatings can be prepared by the layer-by-layer approach that relies on the deposition of positively and negatively charged materials in alternating layers upon a given substrate<sup>14</sup>. The surface should be rinsed with

water after each deposition step to remove excess materials, securing the structural integrity of the final multilayer<sup>14</sup> as well as preventing cross contamination, as shown in Figure 2. This approach is highly effective and very promising in building antimicrobial surface coatings due to its simplicity, flexibility and reproducibility<sup>15</sup>. Building up the layers following this method affords to the coating a high stability due to the presence of strong electrostatic forces between the positively and negatively charged layers. The stability of the coating can be further improved by the use of covalent cross-linking. The thicknesses of the coating can be fine-tuned with respect to the number of bilayers and the pH<sup>16</sup>.

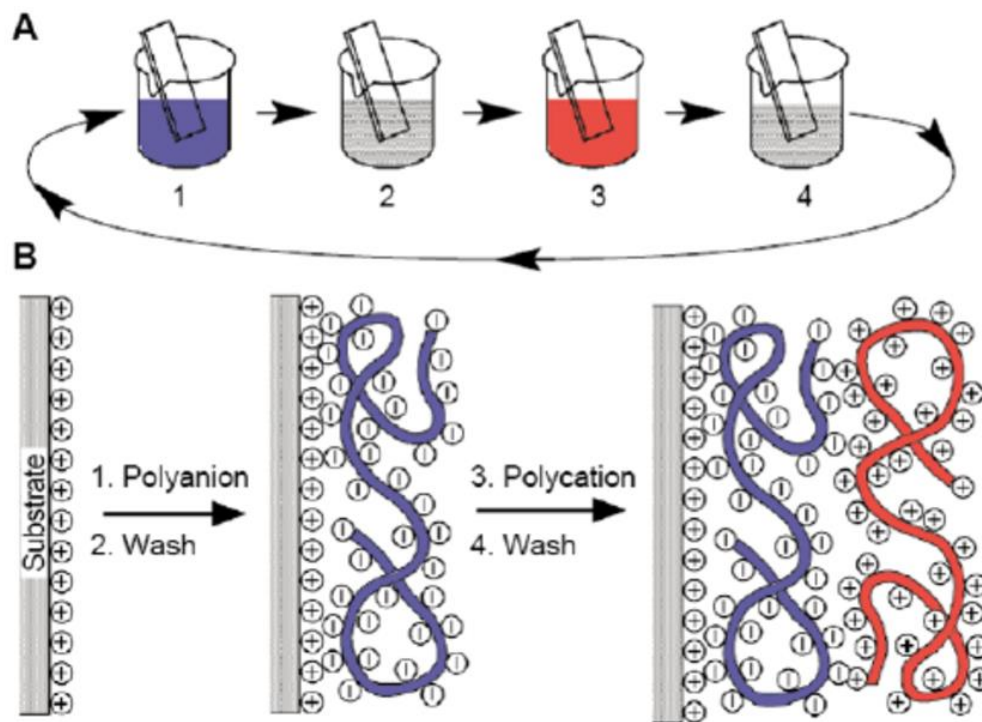


Figure 2. Layer-by-layer assembly from negatively and positively charged solutions on top of the positive base layer added by the spin coater. The part labelled A shows the order of the negative (blue) and positive (red) solutions being added with the washes between, and Part B depicts the build-up of the coating on a given substrate<sup>17</sup>.

A popular variation of this method is based on the spray-coating and the dispersion of the charged particles that is preferable for rough, uneven or larger

surface. This method facilitates the development of uniform coatings comprised of nanoparticles<sup>18</sup>.

Dip layer-by-layer assembly is another variation of this method. During the dip approach, the layers are formed by submerging the surface being coated into a series of at least two or more solutions as shown in Figure 2. The problem with this method is that it requires large amounts of polymer solutions, is time consuming and is not suitable for large surfaces<sup>19</sup>.

Another way in which layer-by-layer coatings can also be formed is by using a spin coating technique to deposit the layers. This method allows the accurate control of the thickness by adjusting the spin speed, spin time and also by controlling the solvent evaporation rate<sup>19</sup>. Spin layer-by-layer assembly is often the method of choice because it is capable of creating bilayers at a fast rate<sup>19</sup>. Using this method also allow microfibers and nanofibers to be coated onto various substrates. Electrospinning works by spinning a polymer solution in to nanofibers<sup>4</sup>. Despite this there are also disadvantages to spin layer-by-layer method for example only one side of the surface can be coated at a time<sup>20</sup>.

### 1.2.2 Other Approaches for Generating Surface Coatings

Chemical vapour deposition is a method for producing coatings whereby a gas-phase reaction of molecules inside a reactor, causes the deposition of the layers onto the surface. This method is useful as it allows the complex substrates to be coated and the films that are produced to be of nanoscale thickness. The thickness of the layer can be adjusted depending on the gaseous reaction and reaction conditions that are used<sup>4</sup>.

Electrochemical methods have also been developed to produce surface coatings. These include methods such as electrochemical deposition and electrochemical polymerization. These methods can be used to amplify the roughness of the surface<sup>4</sup>. Allowing a wider range of potential applications, which rely on surface roughness.

### 1.3 Materials with Antimicrobial Activity

There are many materials that are used or have the potential to be used for antimicrobial application. One example is Nitric oxide. Nitric oxide is produced by the immune system as an antimicrobial in response to a bacterial infection. It is able to give this antimicrobial response due to its oxidizing power. Therefore, it is possible to incorporate nitric oxide into the surface coating where it can be released and used as an antimicrobial agent when the coating is exposed to a reducing agent. Nitric oxide has been shown to act against a broad spectrum of bacteria meaning that the surface coatings into which it is incorporated can have the potential to be used for a wide variety of applications<sup>2</sup>.

Peptides are also regularly used in surface coatings due to their ability to act as an antimicrobial. Peptides with antimicrobial properties can be used in release based coatings as well as being immobilised onto the coating for contact killing. One antibacterial peptide used is Nisin, which has been used for application as an antimicrobial in layer-by-layer coatings in which it is covalently bound. As Nisin is immobilized in the coating it takes action on bacteria through contact killing<sup>2</sup>. *N*-halamines have also been used for application as contact killing in surface coatings. This is because they contain oxidative halides which can directly kill

bacteria upon contact. An advantage of *N*-halamines being used in antimicrobial coatings is that they are able to attack the bacteria without the halogen being released into the surrounding environment<sup>2</sup>.

### 1.3.1 The Use of Nanoparticles for Antimicrobial Surface Coatings

Nanoparticles are particles that are extremely small but possess a large surface area<sup>21</sup>. Their size ranges between 1 – 100 nm<sup>22</sup>. This large surface is beneficial when being used as an antimicrobial as it means there is more surface available for interaction with the bacteria<sup>23</sup>. The surface-to-volume ratio also allow them to change their Physical, chemical and biological properties. This allows them to be adapted to their required applications<sup>24</sup>. Some materials are often made more useful by reducing their particle size, leading them to not only show improved biocompatibility, but also allowing them to be more easily modified to give better performance in their applications<sup>25</sup>. Nanoparticles have been shown to give antimicrobial properties against both gram-positive and gram-negative bacteria<sup>26</sup>.

There are three mechanisms that are suggested for how nanoparticles are able to exhibit antimicrobial activity. The first being through oxidative stress, the second being through metal ion release and the third being through non-oxidative mechanisms. The main processes that are thought to take place during these mechanisms are the disruption of bacteria cell membrane, the generation of a reactive oxygen species, the penetration of the bacterial cell membrane and the disruption of the intercellular functioning. Although these are accepted methods of how the nanoparticles are able to act upon bacteria, the mechanisms are still not fully understood<sup>27</sup>.

One of the most popular nanomaterials used are silver ions, these particles have been shown to exert toxic effects on microbes<sup>26</sup> and are well-used in various fields, which include consumer, food, health care, industrial and medical purposes<sup>28</sup>. It has been stated that silver ions have been shown to have highly promising antimicrobial effects and are more effective in nanoparticle form reducing problems of antimicrobial resistance<sup>25</sup>. One of the ways silver ions are thought to exert antimicrobial activity upon the bacterial cell, is through electrostatic interactions that can take place using positively charged silver ions interacting with the bacteria's negatively charged cell wall<sup>25</sup>. Due to the strong antimicrobial effects shown silver nanoparticles have been used in a number of different applications such as within medical environments, for food storage and even in textile coatings<sup>29</sup>.

Other nanomaterials known for their antimicrobial activity are copper and copper oxide<sup>7</sup>. Copper nanoparticles have been reported to act as an antimicrobial against a broad spectrum of bacteria and fungi including *E.coli*, *S.aureus*, *Pseudomonas aeruginosa* and *Aspergillus flavus*<sup>30</sup>. The broad antimicrobial activity of copper nanoparticles means that they are currently being successfully used in various applications, which include for medical instruments, water treatment and food processing<sup>30</sup>.

Even though metals and their oxides, offer promising antimicrobial effects and are unlikely to cause the development of antimicrobial resistance, there are still concerns about their use due to the potential toxicity to mammalian cells, which the metal nanoparticles may cause<sup>30</sup>. Nanoparticles being used as antimicrobial agents are able to be incorporated into a layered coating, e.g. silver

nanoparticles, Chitosans and *N*-halamines<sup>31-33</sup>, and can then be used effectively against the pathogens it targets, when they come in contact with the surface.

### 1.3.2 Use of Polymer Surfaces

There are many different types of polymers that have antimicrobial properties, which can be applied for the use in surface coatings, such as bioactive polymers and cationic polymers. Bioactive polymers are synthetic or natural polymers that possess properties or have a bioactive material added, which can bring about a biological response or interact with a specific type of living organism<sup>4</sup>. Bioactive polymers can therefore act as an antimicrobial material in various methods, by reducing the adhesion of bacteria<sup>34</sup>. This means, cationic polymers are able to act as antimicrobials, by disrupting the bacterial cell membrane<sup>35</sup>. As most bacteria cell walls are negatively charged, they are able to strongly adhere with the positively charged polymers<sup>4</sup>. Cationic polymers have been reported to give antimicrobial effects against both gram-negative and gram-positive bacteria<sup>36</sup>.

There are many other applications that polymer coatings can be used for such as self-cleaning and anti-icing<sup>4</sup>. Self-cleaning surfaces are surfaces in which dirt particles can be easily picked by water droplets and run away with the water. This is made possible by having minimal surface roughness contact between the roughened surface and the dirt particles which leads to the self-cleaning lotus effect<sup>4</sup>. Anti-icing coatings work by repelling drops of water before they have time to freeze, and a common way to deal with this is to use an anti-icing chemical, however they usually contain toxic chemical and their effects are often short lived<sup>4</sup>.

There are many polymer based coatings that are currently commercially available. Thermoplastics are widely used in antimicrobial coatings, e.g. Talisman 30 and Talisman 30AM, these give rise to tough, hard wearing coatings with a glossy finish that is unlikely to crack, chip or flake. they are available in electrostatic sprays and fluidised bed dipping powders, facilitating its application to any type of large or small surface. Significantly, those coatings can kill 99.9% of certain pathogens<sup>37</sup>. Another thermoplastic used for antimicrobial coatings is commercially known as PPA 571, this gives a glossy coating, which can last for years and can be used in a variety of ways including; lamp posts, fencing, and street furniture to handrails, stadium seat frames and automotive parts. PPA 571 is, to a certain extent, environmentally benign and is free halogens and heavy metals. It is typically applied as fluidised bed dips, electrostatic sprays, flock sprays, extrusion and flame sprays. It is able to prevent the deposition of certain pathogens by a factor of 99%<sup>38</sup>. Polyamides are also well established antimicrobial coatings, with a wide range of applications. Nylon based compositions are applied to a range of surfaces including those used in hospitals and by food processing companies. The coating can be applied to most surfaces, including most metals, polyurethane foams and thermosets<sup>39</sup>.

#### 1.4 Antimicrobial Agents Used in this Study



In this study, different antimicrobial agents were incorporated into the layer-by-layer multisystem in varying combinations.

#### 1.4.1 Chitosan

Chitosan is a polysaccharide formed from beta-(1-4)-linked D-glucosamine and N-acetyl-D-glucosamine, which can be obtained from chitin found in seafood and is produced from the treatment of shrimp and crustaceans with sodium hydroxide<sup>40,41</sup>. Due to the positive charge on chitosan, it can contact-kill a large spectrum of the bacteria, including both gram-positive and gram-negative<sup>42</sup> strains, the method of which has been proposed using three models<sup>42</sup>. The most commonly thought method is that it's the chitosan's cationic nature which gives it its antimicrobial ability<sup>41</sup>. It's thought that the antimicrobial activity takes place due to the interactions between the positively charged chitosan and the negatively charged bacteria cell membrane<sup>42</sup>. This interaction causes the permeability to change, resulting in an osmotic imbalance in the cell, which leads to cell lysis, whereby the leakage of the intercellular electrolytes leads to the destruction of the cell. Chitosan's positive charge also means that it is able to interfere with the microbial growth by interacting with the cells essential nutrients. This method therefore means that the more charged the chitosan, the more significant the antimicrobial affect that will be observed<sup>41</sup>.

The other mechanism that has been proposed is whereby chitosan binds with microbial DNA when it penetrates the nuclei, causing inhibition of mRNA and protein synthesis causing disruption to the cells functions. The final model is where the chelation of metals causes the spore elements, and binding of essential nutrients to the bacteria to be suppressed. This mechanism is more effective when at a high pH as it causes more positive ions being bound to the

chitosan. This means that the chitosan will more readily interact with the negative cell membrane of the bacteria<sup>42</sup>.

In addition, chitosan has shown good biocompatibility, permeability resistance from oxygen and carbon dioxide, and a high ability to form films<sup>43</sup>; all of those are desired characteristics for coating development. The uses of chitosan can sometimes be limited by its properties; such as its low thermal stability and degradation under UV light<sup>43</sup>.

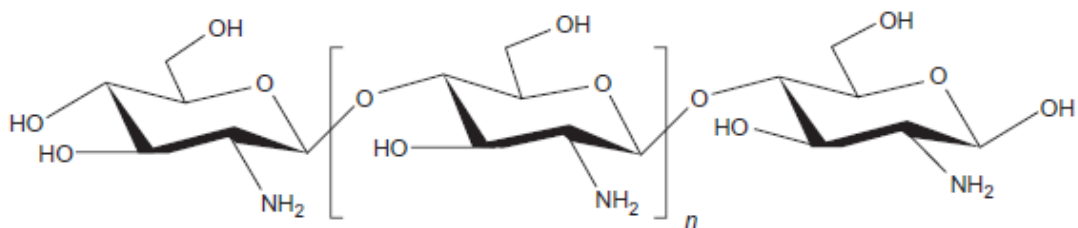


Figure 3. The structure of chitosan<sup>40</sup>

#### 1.4.2 Lysozyme

Lysozyme is another antimicrobial agent that is incorporated into layer-by-layer coatings. Lysozyme is an enzyme, which is used as an antibacterial against food spoilage as well as pathogenic microorganisms<sup>44</sup>. It is also capable of catalysing the hydrolysis of the peptidoglycan in the bacterial cell wall. This means that it is capable of causing significant damage to the bacterial cell wall, as peptidoglycan is the main component of the cell wall in gram-positive bacteria. In gram-positive bacteria, peptidoglycan forms the thick cell wall of the bacteria, whereas in gram-negative bacteria peptidoglycan forms a thin cell wall<sup>45</sup>. When bacteria is exposed to lysozyme it causes damage to peptidoglycan that then leads to the rupturing

of the cell wall and the inflow of water into cell. This increases the pressure inside the cell and eventually causes cell lysis<sup>45</sup>. Lysozyme does not usually show antimicrobial activity against gram-negative bacteria unless the lysozyme is modified, this is because gram-negative bacteria has an outer layer of lipopolysaccharide around the peptidoglycan layer which prevents lysozyme from accessing the peptidoglycan layer making gram-negative bacteria more resistant to lysozymes antimicrobial action<sup>46</sup>. Figure 4, shows Lysozyme interacting with the peptidoglycan in gram negative bacteria.

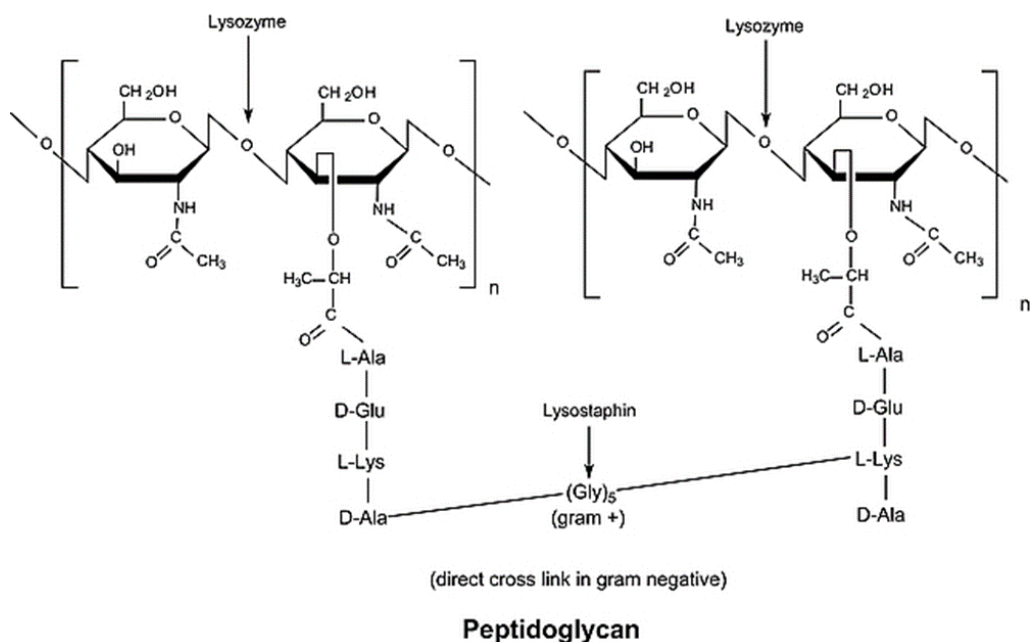


Figure 4. *The interaction between the peptidoglycan in gram negative bacteria and lysozyme*<sup>47</sup>

### 1.4.3 Nafion

Nafion is a type of polymer that is a perfluorosulfonated isomer membrane, which was first commercialized by DuPont de Nemours<sup>48</sup>. This was formed by

hydrolysing the precursor sulfuryl fluoride, forming the perfluorosulfonate polymer Nafion. Currently Nafion is formed by being casted from suspension<sup>49</sup>, it is made up of a fluorocarbon backbone with long pendant perfluorosulfonated ionic pendant groups. It is these sulfonated pendant group that have properties of ion-exchange. Other properties include thermal, chemical and mechanical stability<sup>50</sup>. The Nafions sulfonic side chain group dissociates when hydrolysed in solution. This means that the polymer left behind is negatively charged<sup>51</sup>. This side groups can be seen in Figure 5 below. The negative charge on Nafion means that it is able to be used as the negative layer in the multilayer systems of the surface coatings. A polymer with the opposite charge (positive) to Nafion can then be layered across the Nafion membrane coating<sup>49</sup>.

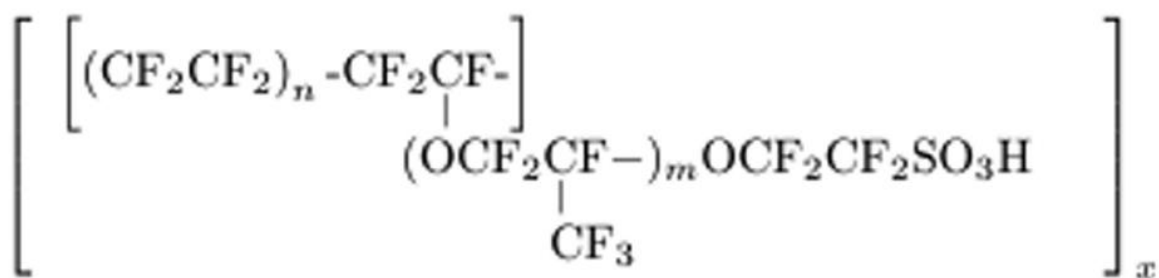


Figure 5. The chemical structure of Nafion<sup>49</sup>

#### 1.4.4 Polyvinylpyrrolidone

Polyvinylpyrrolidone (PVP) is another antimicrobial agent that was used in forming the layer-by-layer coatings. PVP is a hydrophilic synthetic polymer which can be made by free radical polymerisation from its monomer *N*-

vinylpyrrolidone<sup>40,52</sup>. It is known to have good biocompatibility<sup>52</sup>. Due to being non-toxic PVP is able to be used for biomedical applications<sup>52</sup>. PVP can be used along with other biocompatible materials such as iodine. PVP is added to iodine enabling it to be used in items such as liquid soaps, surgical scrubs and even some ointments due to its disinfectant properties<sup>40</sup>.

PVP is also used as a synthetic thymus-independent type 2 antigen that immune response is T-cell regulated<sup>53</sup>. It is used in a lot of animal immunological studies with it being identified to successfully bind with antibodies<sup>53</sup>.

One of the disadvantages found with PVP coatings is that they are known to degrade, via oxidation, under UV light and oxidizing environments<sup>54</sup>.

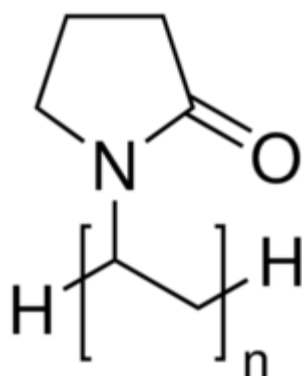


Figure 6. The structure of PVP

#### 1.4.5 QPDMAEMA – PLMA Diblock

The QPDMAEMA – PLMA Diblock is also used as an antimicrobial agent for the layer-by-layer coatings. PDMAEMA – PLMA Diblock is a co-polymer based on lauryl methacrylate (PLMA) and 2-dimethylaminoethyl methacrylate (DMAEMA; we used the quaternised diblock (N+/I-). QPDMAEMA - PLMA is made from the monomers 2-Dimethylaminoethyl Methacrylate and Lauryl Methocrylate to make

PDMAEMA-PLMA-Diblock, which is then quarternised, to form QPDMAEMA – PLMA Diblock and is dissolved in distilled water, to form the solution used for layering the plate.

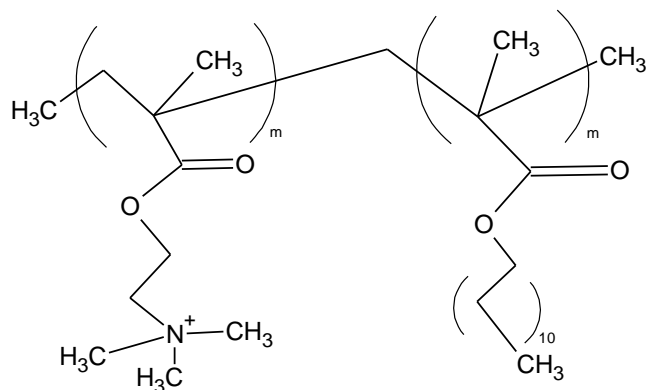


Figure 7. The structure of QPDMAEMA-PLMA diblock copolymer

### 1.5 Gram-Positive and Gram-Negative Bacteria

The surface coatings are tested against two different types of bacteria; *Escherichia coli* (*E.coli*), which is a gram-negative and *Staphylococcus aureus* (*S.aureus*) which is gram-positive. Gram-positive bacteria have a thick and rigid structure due to containing numerous layers of peptidoglycan in its cell wall, as well as containing teichoic acids. There are two types of teichoic acid that can be found in gram-positive bacteria; lipoteichoic acid and teichoic wall acid, which has a negative charge, regulating movement of cation across the cell membrane. There is no outer membrane present in gram-positive bacteria<sup>55</sup>. The gram-positive bacterium *S.aureus*, grows in an optimum temperature of 37°C and optimum pH of 6-7, although, is capable of forming in temperatures of 7-48°C and pH of 4-10. *S.aureus* form biofilms mainly on surfaces where food is prepared<sup>56</sup>.

Gram-negative bacteria have fewer peptidoglycan layers that are made up of lipopolysaccharides, lipoproteins and phospholipids, which means they are not easily affected by antibodies, enzymes, metals, detergents and salts, although containing a thinner cell wall means they are more susceptible to breakage. Unlike gram positive bacteria, gram-negative bacteria does not contain any teichoic acid. Periplasm is present in gram-negative bacteria, which acts as a compartment for proteins to be stored in. These compartments are found all across the peptidoglycan layer. It is this cellular compartmentalisation that has the potential to be protected against enzymes that would normally be harmful to the bacteria<sup>55</sup>. The components of the gram-negative bacteria's envelope is either made in the cytoplasm or the inner surface of the inner membrane<sup>55</sup>. The outer membrane gives the gram-negative extra protection<sup>55</sup> and is needed due to the gram-negative bacteria having fewer peptidoglycan layers. The gram-negative bacterium *E.coli* is a rod like, with projections of peritrichous flagella, which enables it to have motion<sup>57</sup>. It often has an outer membrane surrounded by a capsule made up of polysaccharides. There are several different types of *E.coli*, which can either be pathogenic or non-pathogenic. Non-pathogenic can be found in the gut and is harmless to humans. However pathogenic *E.coli* which can be found in contaminated water and food has the potential to be very harmful to humans, potentially causing urinary tract infections, infections to the central nervous system and gastroenteric diseases<sup>58</sup>. Silver nanoparticles are one of the many materials that can be used as an antimicrobial and has shown to effectively kill *E.coli* and *S.aurues*, when used for contact and release killing layer-by-layer films<sup>2</sup>.

# Chapter Two

## Experimental section

### 2.1 Materials

Citric Acid, Di Sodium Phosphate, and Polyvinylpolyiodine were all purchased from Alfa Aesar, Haverhill, Massachusetts, United States. Nafion was purchased from Ion Power, Munich, Germany. Acetone, Ethanol, and Lysozyme from chicken egg white were purchased from Sigma-Aldrich, Poole, Dorset, UK. QPDMAEMA - PLMA was synthesised by the research group of Professor Asterios Pispas, National Hellenic Research foundation, Athens, Greece.

### 2.2 Methods

Predisposed Nafion was made from 1ml Nafion in 30ml of ethanol. Deposited Nafion: 1ml of Nafion in 40ml of distilled water. Lysozyme was made by 0.015g being dissolved in 6.2 buffer solution made up to 15g. 6.2 buffer solution was made from 2.101g of Citric Acid dissolved in 100ml of distilled water and 2.84g of Di Sodium phosphate dissolved in 100ml of distilled water. Both combined to a solution to make a 6.2 pH buffer solution. Roughly 33.90ml of Citric Acid and 66.10ml of Di sodium phosphate. A Jenway 3505 pH meter was used. Chitosan was made by 0.1g of chitosan being dissolved in 100ml of 0.1M acetic acid and sonicated for an hour to dissolve the chitosan powder. QPDMAEMA – PLMA



Diblock was made by 0.0302g of QPDMAEMA – PLMA Diblock in 45ml of distilled water. PVP was made by 0.15g of PVP being dissolved in 45ml of distilled water.

### 2.3 Quartz Crystal Microbalance with Dissipation Monitoring

A Quartz Crystal Microbalance Dissipation was used to coat the gold crystal plates. Crystal plates were washed by dipping the plates in Pluronic solution, followed by rinsing with acetone and distilled water. The plates were then left to dry, before being pre-coated with a Nafion/ethanol solution, by placing a few drops of the solution onto the crystal plate and then being either air dried or dried on the Ossila spin coater, for 60 seconds. Ossila spin coater works by spinning the disk at high speeds causing the ethanol to evaporate to leave a thin even coat of Nafion on the crystal plate<sup>59</sup>. The plate was then placed in the Quartz crystal microbalance with dissipation monitoring (QCMD), where the layers are deposited onto the crystal. The temperature on the QCMD was set to 22 °C, as this is close to an average room temperature. This avoids the coatings, which are already at room temperature, experiencing any temperature change when injected into the QCMD. The plate is then allowed to stabilise for about an hour before the layers are deposited onto the crystal.

The Layer-by-layer coatings are deposited onto the crystal disk using QCMD, where QCMD measures changes in the resonance frequency ( $\Delta F$ ) and the dissipation ( $\Delta D$ ), which is a measurement of the energy loss from the system<sup>60</sup>. The QCMD works by taking measurements of the mass of the deposits on the crystal plate by recording the vibrations, which are generated by the oscillating piezoelectric crystal quartz plate. The quartz is usual AT cut as it enhances certain desirable properties such as, the ability to remain stable in fluctuating

temperatures. The crystal is placed between two metal electrodes, then an alternating electric current is applied across the electrodes, causing the crystal to oscillate<sup>60</sup>. The frequency of the sensor changes, as the oscillating mass changes. When a layer is added to the plate, the frequency decreases proportionally. For this reason, the quartz crystal is considered a highly precise and stable oscillator. The QCMD measures changes based on Sauerbrey's equation (Eq. 1), which is used to calculate the mass of the layers:

$$\Delta m = C/n\Delta f \quad \text{Eq. (1)}$$

Where  $n$  is the harmonic number,  $\Delta f$  is the change in frequency,  $\Delta m$  stands for the changes in mass deposited and  $C$  is the crystal sensitivity depending on the thickness and density of the crystal (Eq. 2):

$$C = T_q P_q / f_0 \quad \text{Eq. (2)}$$

Where  $T_q$  = thickness of the quartz and  $P_q$  = density of the quartz and equals

The calculation used to measure the dissipation factor ( $D$ ) (Eq. 3) is:

$$D = E_d / (2\pi E_n) \quad \text{Eq. (3)}$$

This is where  $E_d$  and  $E_n$  refers to the energy dissipated and stored in a single oscillation cycle<sup>60</sup>.

The assumptions made by Sauerbrey equation are:

1. The absorbed mass must be small in relative to the mass of the quartz crystal
2. Mass absorbed is rigidly absorbed
3. Mass absorbed is evenly distributed over the active area of the crystal<sup>60</sup>

The QCMD is capable of measuring the amount of protein that is absorbed onto the surface. From this it can be determined if the surface is resistant to the absorption of the protein or allows the protein to absorb readily onto it. The

absorption of the protein may be wanted or unwanted depending on the protein and the outcome of its absorbance. In this study Nafion, lysozyme, chitosan, QPDMAEMA - PLMA and PVP were deposited onto the crystal by the QCM-D in the layer-by-layer technique.

When placed in the QCM-D the crystal plate is first stabilised for an hour before any deposits are made onto the crystal. This is to allow the crystal to reach a stable frequency. After the stabilisation process is finished water is first run through the QCM-D onto the crystal plate to allow the baseline establishment for the wet crystal. At this point the crystal is ready for the build-up of a multilayer and the first building block is injected to the system. After a stable frequency reading is established, the crystal is washed with water to remove any loosely bound molecules. A succession of negatively/positively layer deposition in an alternating fashion allows the construction of (N/L)x6, (N/C)x6, (N/M)x3, (N/P)x3, (N/L/N/C)x2, (N/P/N/L)x1 and (N/P/N/C)x1. In this study, Q-Sense QCM-D was used as the QCM-D.

#### 2.4 Antimicrobial tests

All antimicrobial tests were conducted by Ella Gibbons, Ph.D Student, from the School of Pharmacy and Biomedical Sciences, University of Central Lancashire. The method used to test antimicrobial activity was adapted from Zhong et al<sup>51</sup>. Bacteria cultures were grown in 25 ml nutrient broth in a Chronical flask and shaken in an orbital shaker for 24 hr at 200 rpm and 37 °C. These were repeatedly centrifuged and the supernatant removed followed by the addition of Ringers solution. The re-suspended culture was then diluted to the desired level.

The disks were placed into 12 well plates that have been lined with aluminium foil for easy transportation of the plates, as shown below in Figure 8. The aluminium is autoclaved at 80 °C, for sterilisation to avoid any contamination of the samples. Disks are first inoculated with 200µl of bacteria culture and then incubated in at 37 °C for 20hrs, before being placed in Ringer solution, followed by sonication and dilution to a factor of 1 in 10, repeated up to 4 times. Then 100 µl of the culture to be spread onto each plate in triplicate. Plates were incubated for 24 hrs at 37 °C and the number of Colony Forming Units (CFU) were counted and then recorded. The bacteria used were *E.coli* and *S.aureus*<sup>51</sup>.

The results from the antimicrobial testing, showed the amount of the bacteria that decreased on the plate after an incubation period. The percentage decrease is given as a logarithm and is determined by recording the number of colony forming units after incubation of 100µl of the culture on the nutrient agar and tested against a control disk that was not coated in the multi-layer component, but was incubated with the same bacteria. The colony units were manually counted, with the aid of a colony counter.

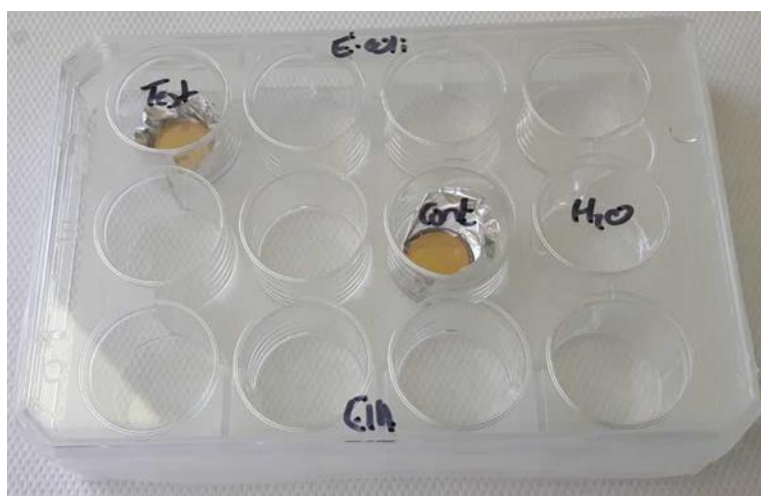


Figure 8. The coated disk and the control being cultured with *E.Coli* to measure the percentage decrease in the *E.Coli*.

## 2.5 Fourier Transform Infrared Spectroscopy

FT-IR works by using IR radiation to determine the bonds present within the sample. Different types of bonds will vibrate at different wavelengths. These vibrations are shown as peaks on spectra produced. The spectra can then be used to identify the bonds present in the sample<sup>61</sup>.

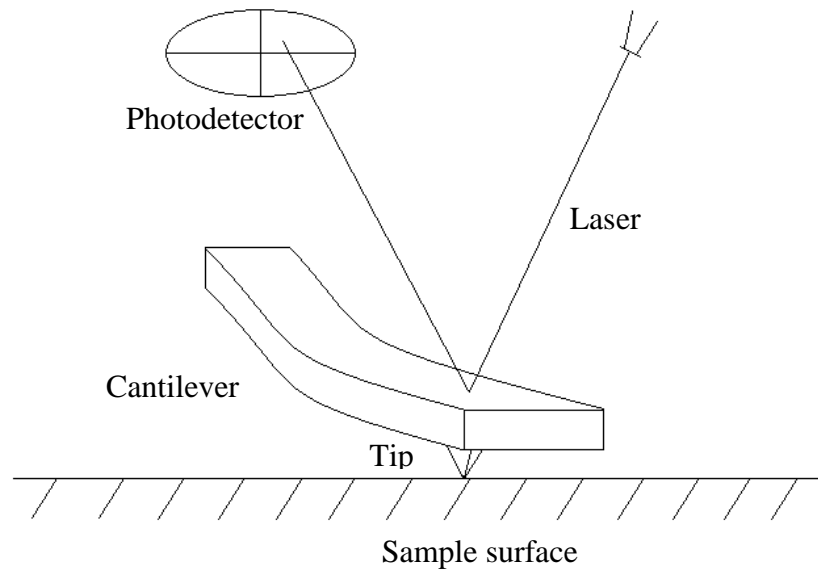
FT-IR spectra of the materials used as layers for the assemblies (e.g. Nafion, lysozyme, chitosan, etc) were compared to the spectra collected for their binary blends (e.g. Nafion/lysozyme, Nafion/chitosan, etc). Pronounced peak shifts between the unbound and the bound state were identified and were considered as evidence for extensive particle-particle interactions. To prepare the blends, the materials were first mixed in water and their precipitant was freeze-dried.

In this study a Thermo scientific Nicolet IS5 FT-IR machine was used.

## 2.6 Atomic Force Microscopy

Another method of analysis is Atomic Force Microscopy (AFM) and is used to obtain images of the surface showing the surface morphology, roughness and thickness of the multilayers<sup>50</sup>. AFM allows a topographic characterization of the surface that is being studied and allows molecular scale features to be identified in real time<sup>62</sup>. AFM works by a probe, called a cantilever, scanning across the surface of the sample that's being analysed, magnifying the image into the nanometre scale. A laser beam is reflected off the back of the cantilever onto a photodetector, meaning that any small changes in the cantilever can be detected

by the photodetector<sup>63</sup> as shown in the diagram in Figure 9. These changes are responded to by a feedback control system, which is where the information can



be used to determine the topological height changes on the surface<sup>62</sup>. This information is then used to create an image of the surface, that is being analysed.

Figure 9. An image of the AFM system

## 2.7 Contact angle measurements

Contact angle measurements were taken to determine how the surfaces wetting ability as well as how hydrophobic or hydrophilic the surface was. Contact angle of a surface is measured by placing a droplet of water onto the surface, the angle that the droplet sits at is measured. If the contact angle of the droplet is less than  $90^\circ$  it means the surface is readily wetted<sup>64</sup>. If the angle of the droplet is at greater than  $90^\circ$  it means that there is minimal contact between the droplet and the

surface and the surface is not wetted readily<sup>64</sup>. If the contact angle is at  $0^\circ$  then it means, there is complete wetting of the surface<sup>64</sup>.

From this information the surface can be described as being either hydrophilic or hydrophobic. A lower the contact angle suggests a more hydrophilic nature of the surface, meaning the surface contains more polar groups, allowing the water to readily interact with its surface, whilst the higher the contact angle suggests a more hydrophobic nature meaning that the water doesn't readily interact with the surface<sup>65</sup>. When the contact angle is above  $150^\circ$  there is almost no contact between the droplet and the surface meaning that the surface can be described as superhydrophobic. This effect of super hydrophobicity is known as the Lotus effect<sup>66</sup>.

The formation of biofilms happens due to the initial attachment of bacteria onto the surface, therefore coatings that prevent adhesion of the bacteria onto the surface are usually more hydrophobic as they don't allow materials to easily interact with their surface<sup>4</sup>.

The method we use to measure the contact angle of the surfaces is the sessile drop technique as shown in Figure 10. In this technique an image of the water droplet on the surface is taken using a camera, which is fixed into position to give an accurate image of the droplet from which the angle can be calculated. The image is then shown on the screen, where it can be analysed giving the contact angle at which the water droplet sits on the surface. From this information the surfaces roughness, wettability, hydrophilicity and hydrophobicity nature can be analysed<sup>65</sup>.

In this study a FTA 1000 surface tension measurement machine was used which uses the software FTA32.

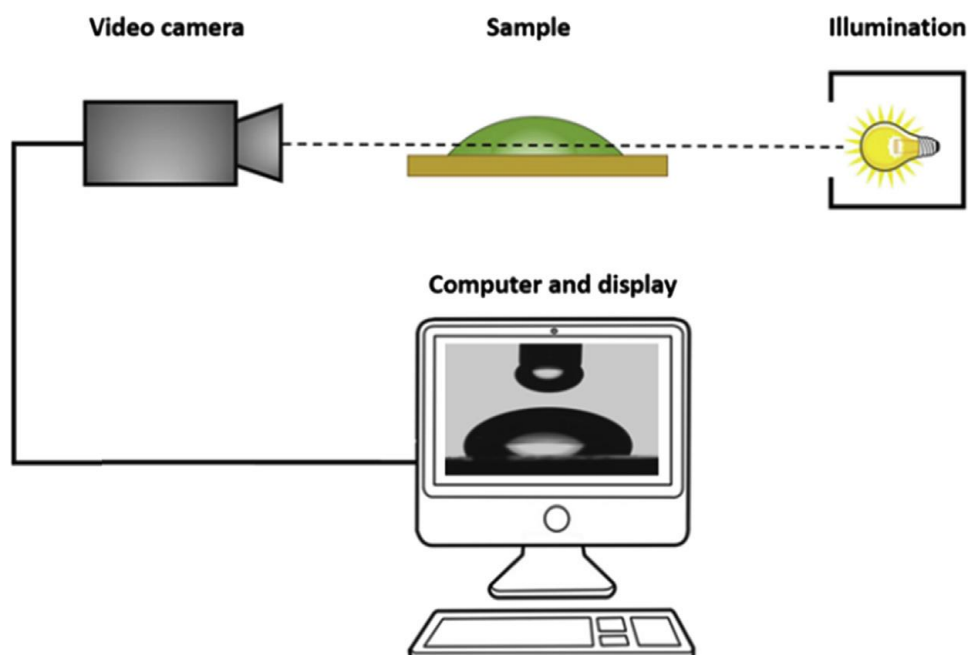


Figure 10. The setup machine of the sessile drop technique<sup>65</sup>.

There are many different factors that can affect the angle of the droplet, such as heterogeneity, surface roughness, particle size and particle shape<sup>65</sup>. One of the main reasons for the effect of the surface heterogeneity is the presence of impurities<sup>67</sup>. Heterogeneity factors are usually unavoidable<sup>65</sup>. The surface roughness influences the contact angle measurement as it changes the spreading and wetting of the water droplet<sup>65</sup>. The rougher the surface, the more likely it is that the surface will have increased hydrophobic<sup>68</sup>. The size and shape of the particles on the surface is an important factor affecting the contact angle as they affect the surface area and roughness<sup>65</sup>. The higher the contact angle and more hydrophobic the surface, the more likely the surface is to act as an effective antimicrobial surface as the bacteria is less likely to adhere to the surface<sup>68</sup>.



## 2.8 UV-Vis spectroscopy and transparency

Ultraviolet-Visible (UV-Vis) is an absorption spectroscopy technique, which works by passing light, within the ultraviolet-visible spectral region, through the samples and measuring the amount of light that is absorbed. The technique measures absorption at different wavelengths in the near ultraviolet radiation (180-390nm) and visible radiation (390-740nm) regions of the electromagnetic spectrum<sup>69</sup>. When radiation energy from within the UV-Vis range is absorbed by molecules, it causes the electron excitation, allowing electronic transition.

The relationship between the amount of radiation absorbed and the concentration of the analyte is known as Beer-Lambert's Law and is shown in the following equation:

$$A = \epsilon \cdot b \cdot c \quad \text{Eq. (4)}$$

where  $A$  is the absorbance of the solution,  $\epsilon$  is the molar absorptivity ( $\text{l mol}^{-1} \text{cm}^{-1}$ ),  $b$  is the path length of radiation through the absorbing medium (cm), and  $c$  is the concentration  $\text{mol l}^{-1}$ <sup>70</sup>.

The transparency of the successful coatings was measured using UV-Vis spectroscopy. Initially, the cuvette was coated using the multilayer system of choice, via the dip-layer method. A blank cuvette is measured to act as the blank control standard, in order to determine, whether the coating provided transparency. Measuring the amount of absorption indicates how transparent the coatings are, where coatings that are more transparent, will give an absorbance value lower than coatings that are less transparent. UV-Vis analysis was performed in this study using a Biochrom WPA Lightwave II UV-Vis spectrophotometer.

# Chapter Three

## Results and Discussion

### 3.1 Nafion/ lysozyme and Nafion/chitosan assemblies

#### 3.1.1 Fourier-Transform Infrared Spectroscopy (FT-IR)

An aqueous dispersion containing Nafion and lysozyme was freeze dried and the corresponding FTIR spectrum was compared with the spectra of the individual components in Figure 11.

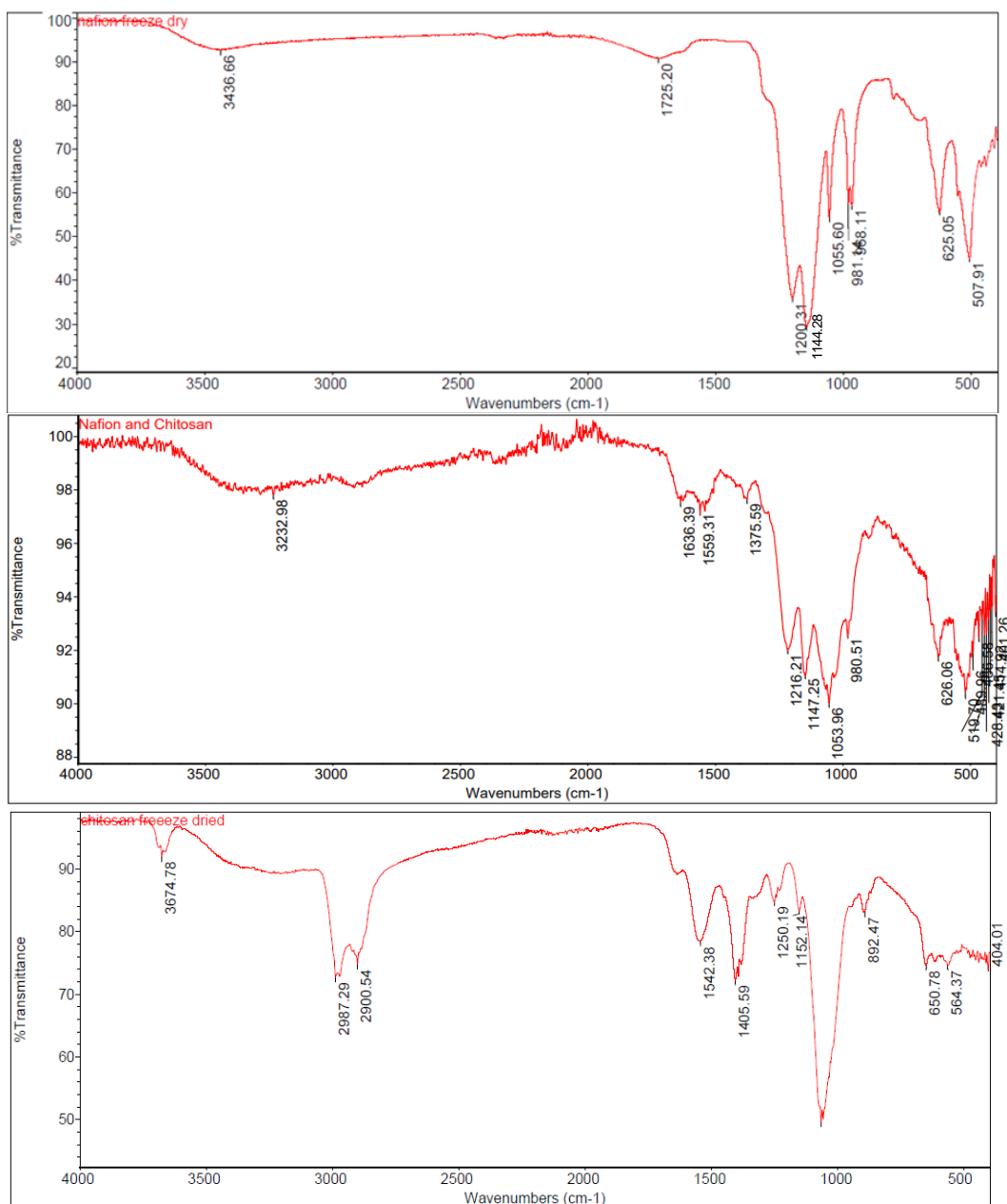


Figure 11. FT-IR spectra for Nafion (upper), Nafion/lysozyme blend (middle) and Lysozyme (lower).

The FT-IR spectrum for Nafion confirms the presence of C-F bond, as shown by the peak at  $1055\text{ cm}^{-1}$ . In Nafion and lysozyme spectrum the peak for the C-F bond is still present but at  $1054\text{ cm}^{-1}$  instead.

The Nafion spectrum also shows a peak for the peaks at  $1144\text{ cm}^{-1}$ , showing the C-F alkyl halide. This peak is also shown in the Nafion-lysozyme spectra by the peak at  $1147\text{ cm}^{-1}$ . The C-O group is shown in the Nafion spectrum at  $1200\text{ cm}^{-1}$ . This is shown in the spectrum for the Nafion-lysozyme blend at  $1211\text{ cm}^{-1}$ . In the lysozyme spectrum peaks for the C=O group is shown at  $1644\text{ cm}^{-1}$  and  $1236\text{ cm}^{-1}$ . These groups are still seen in the Nafion-lysozyme blend spectrum at  $1653\text{ cm}^{-1}$  and  $1211\text{ cm}^{-1}$ . The peak at  $1531\text{ cm}^{-1}$  in the lysozyme spectra and  $1521\text{ cm}^{-1}$  in the Nafion-lysozyme blend structure show the C=C bond. Lysozyme can also be identified in the FT-IR spectra for lysozyme by the peak at  $3288\text{ cm}^{-1}$ , which suggests the presence of either an O-H group or an N-H group. As well as the peak at  $2963\text{ cm}^{-1}$ , which shows the C-H bond.

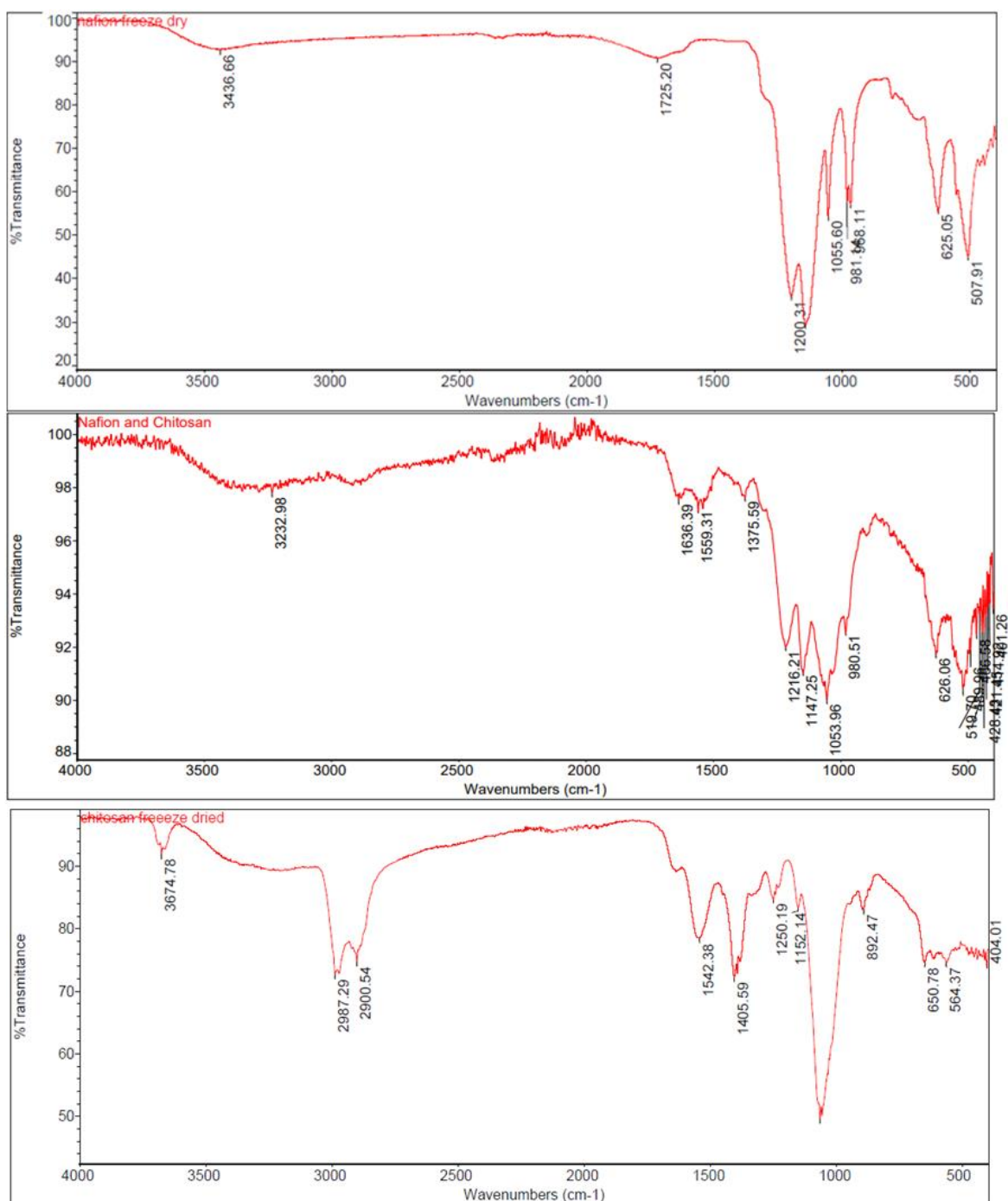


Figure 12. FT-IR spectra for: Nafion (upper), Nafion/chitosan blend (middle), chitosan (lower).

Likewise, the FT-IR spectrum of the freeze dried Nafion/chitosan blend is compared with the spectra of its unbound components in Figure 12. For Nafion, the FT-IR peaks at  $1144\text{ cm}^{-1}$  and  $1055\text{ cm}^{-1}$  are associated to the alkyl halide group C-F and the peak at  $1200\text{ cm}^{-1}$  is associated to the C-O ether group. These peaks can be identified in the Nafion-chitosan blend spectrum at  $1147\text{ cm}^{-1}$ ,  $1053$

cm<sup>-1</sup>, 1200 cm<sup>-1</sup>, respectively. With respect to chitosan, the peak at 1152 cm<sup>-1</sup> is the signature of the C-O bond and the peak at 2900 cm<sup>-1</sup> arises from the C-H alkane bond. The peak at 3674 cm<sup>-1</sup> shows the identity of both N-H amine bond and O-H bond. This peak is still identified on the spectrum of the blend by the peak at 3232 cm<sup>-1</sup>. The peaks for the C-F placed on the backbone of Nafion, do not show any major shifts when interacting with lysozyme and chitosan. In contrast, certain polar groups in Nafion show pronounced peak shifts in Nafion/lysozyme and Nafion/chitosan blends. These interactions are consistent with the formation of a precipitant upon mixing Nafion with lysozyme, as well as Nafion with chitosan.

### 3.1.2 QCM-D

A number of multi-component layer-by-layer coatings were successfully designed and synthesised using the QCM-D. The coatings successfully made were as follows:

(N/L)x6

(N/C)x6

(N/L/N/C)x2

(N/M)x3

(N/P)x3

(N/P/N/L)x1

(N/P/N/C)x1

Each type of layer-by-layer coating was prepared at least 4 times so that different types of analysis (AFM, contact angle, antimicrobial studies) could be conducted.

The graphs produced from the samples run, such as the one shown in Figure 13, showed the change in resonance frequency  $\Delta f$  (blue line) and  $E_d$  (red line) as a function of time, during the build-up of the multilayer systems. The arrows on the graph point to the time, where a given material is being introduced to the system.

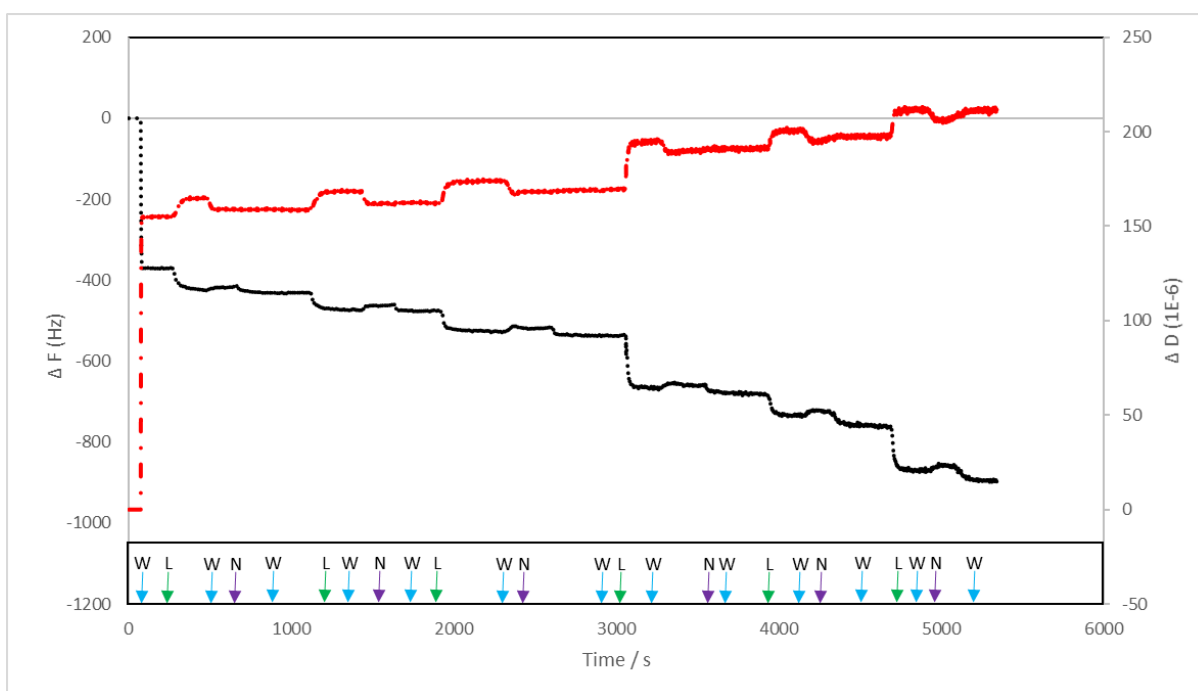


Figure 13. QCMD graph for layer-by-layer deposition of (N/L)x6. The letters W,L, N denote the injection of water, lysozyme and Nafion solutions, respectively.

When water is introduced to the Nafion pre-coated crystal, a significant frequency drop signifies the ample hydration of the Nafion membrane. The effect is directly related to the presence of water channels within the Nafion transport that are able to accommodate large quantities of water. It is now well established that Nafion undergoes microphase separation into polar/non-polar domains, with the robust Teflon like backbone, offering mechanical support to a tubular system of

interconnected water channels. Moreover, Nafion in its vicinity with water undergoes major molecular rearrangements, so that its hydrophilic domains maximise their contact with the polar solvent. This allows the polar groups in Nafion to interact with the polar groups present in water<sup>71-74</sup>.

When lysozyme is added, it interacts with the Nafion through electrostatic interactions due to lysozyme being positively charged and the Nafion being negatively charged. Lysozyme is able to maintain electrostatic interactions within the layer-by-layer system when between pH 1-11<sup>75</sup>. Lysozyme is therefore dissolved in a buffer solution causing it to maintain a pH of 6.2 throughout this study.



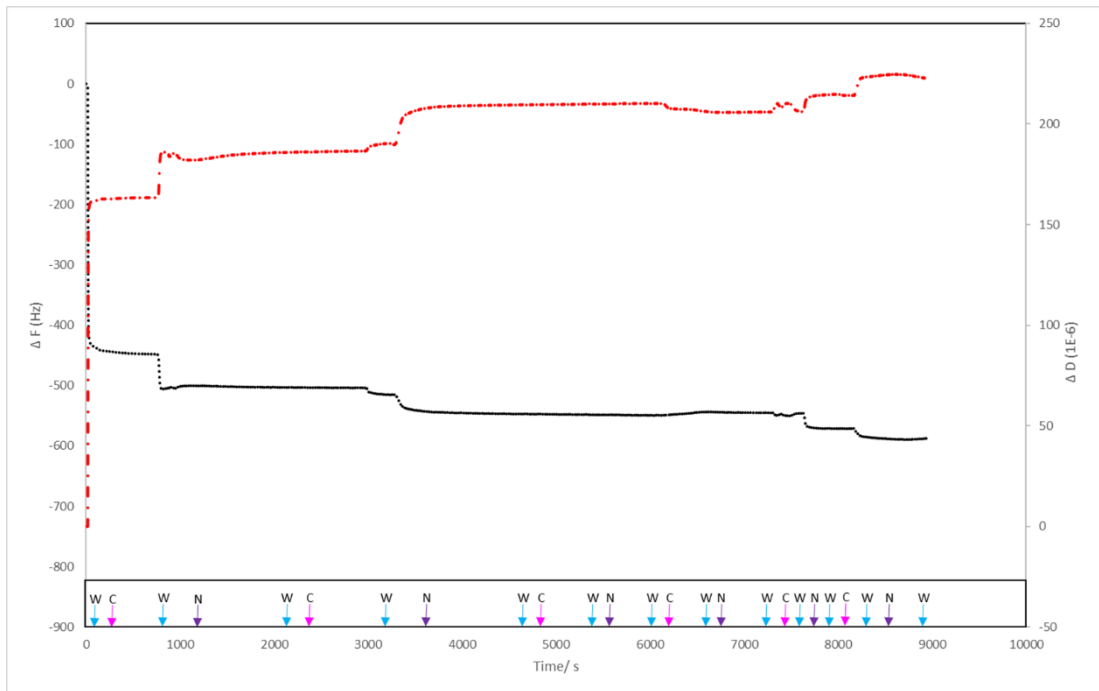


Figure 14. Layer-by-layer deposition of (N/C)x6. The letters W, C,N denote the injection of water, Nafion and chitosan respectively.

The graph in Figure 14 shows the layer-by-layer deposition for a (N/C)x6. The water and the Nafion interact with each other in the same way as previously described in Figure 13, but, chitosan is used as the positive layer instead of lysozyme.. Like lysozyme, chitosan is also positively charged<sup>2</sup>and can also form electrostatic interactions with Nafion, allowing it to strongly absorb onto the Nafion.

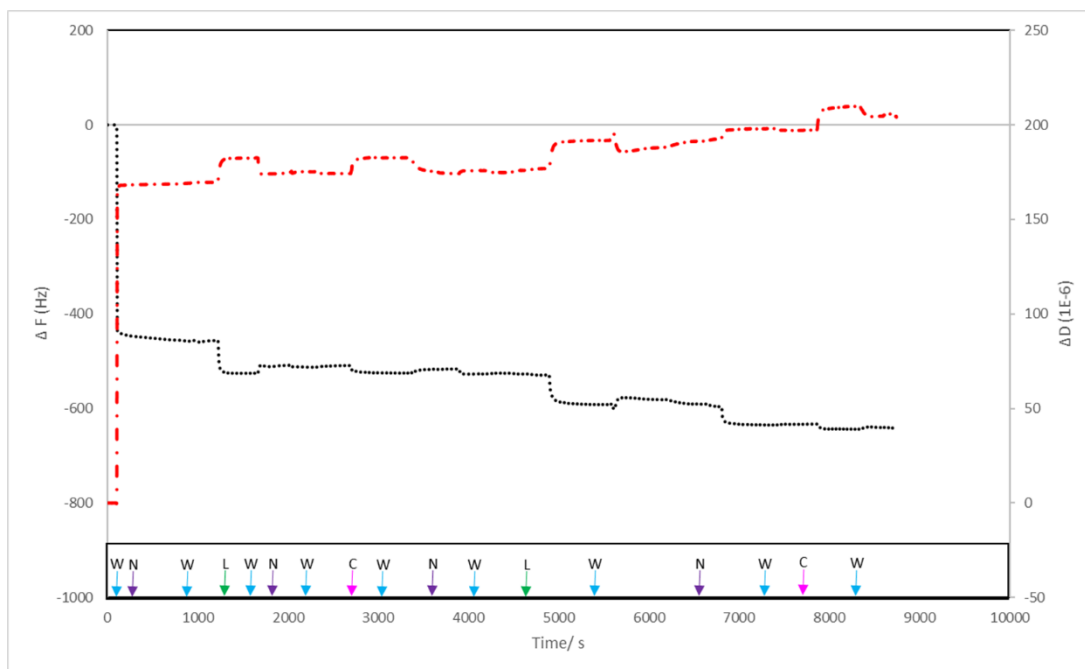


Figure 15. *Layer-by-layer deposition for (N/L/N/C)x2. The letters W ,N,L,C denote the injection of water, Nafion, lysozyme and chitosan, respectively.*

This graph in Figure 15 show the layer-by-layer deposition of (N/L/N/C)x2. The interactions between the Nafion and the water are the same as previously described with Figure 13 where the positive layer, in this layer-by-layer system is an alternate between lysozyme and chitosan, both of which are attracted to the negatively charged Nafion.

### 3.1.3 Antimicrobial testing

Figure 16 shows the percentage reduction of *E.coli* and *S.aureus* colonies, incubated with the coated surfaces, compared to the uncoated blank samples.

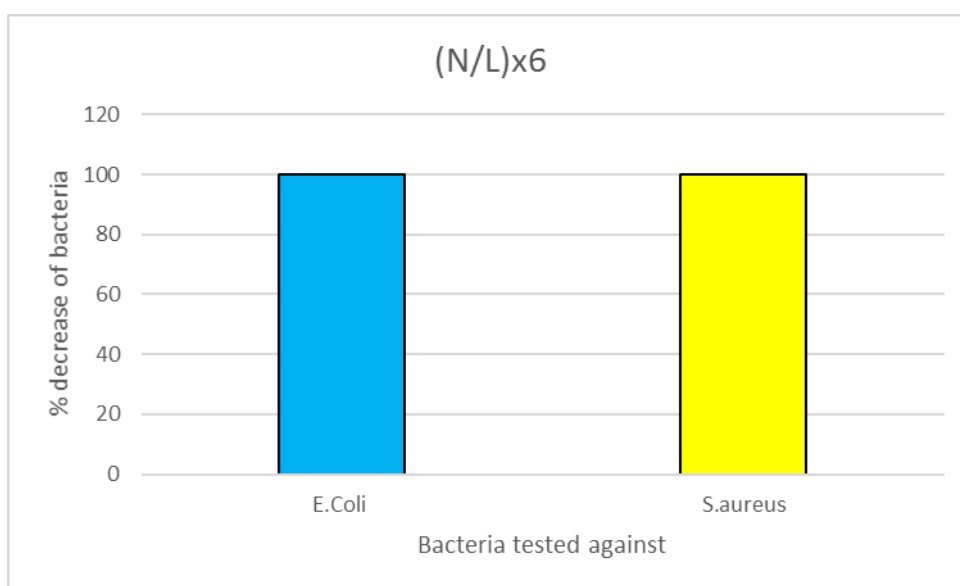


Figure 16. Percentage decrease in *E.coli* and *S. aureus* bacteria incubated with (N/L)x6 coating.

As shown in Figure 16, the (N/L)x6 induced an average percentage decrease of 99.994% against *E.coli* and an average percentage decrease of 99.991% against *S. aureus*, indicating a remarkable antimicrobial activity.

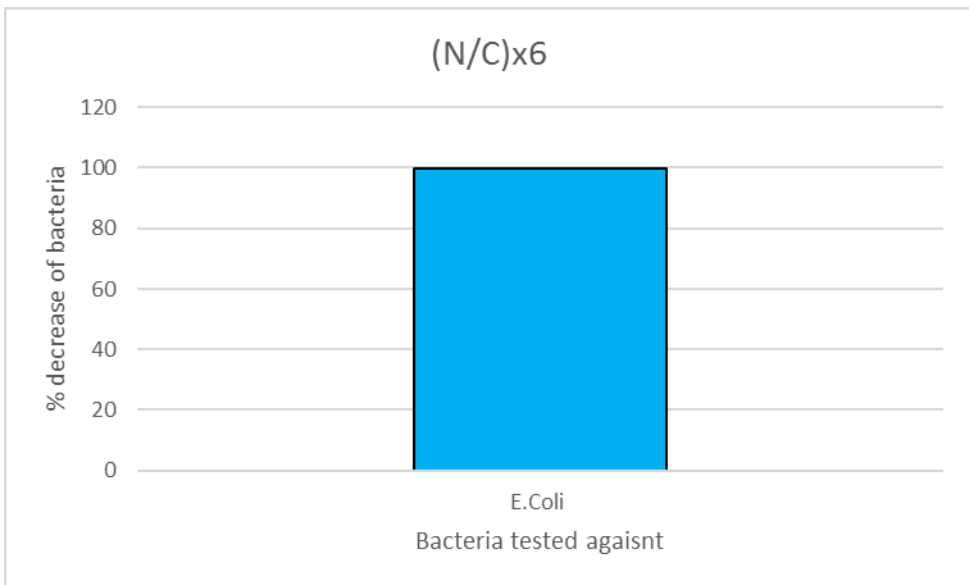


Figure 17. Percentage decrease in *E.coli* bacteria when tested against the (N/C)x6 coating.

Figure 17 indicates that (N/C)x6 imparts 99.9% reduction of *E.coli* population.

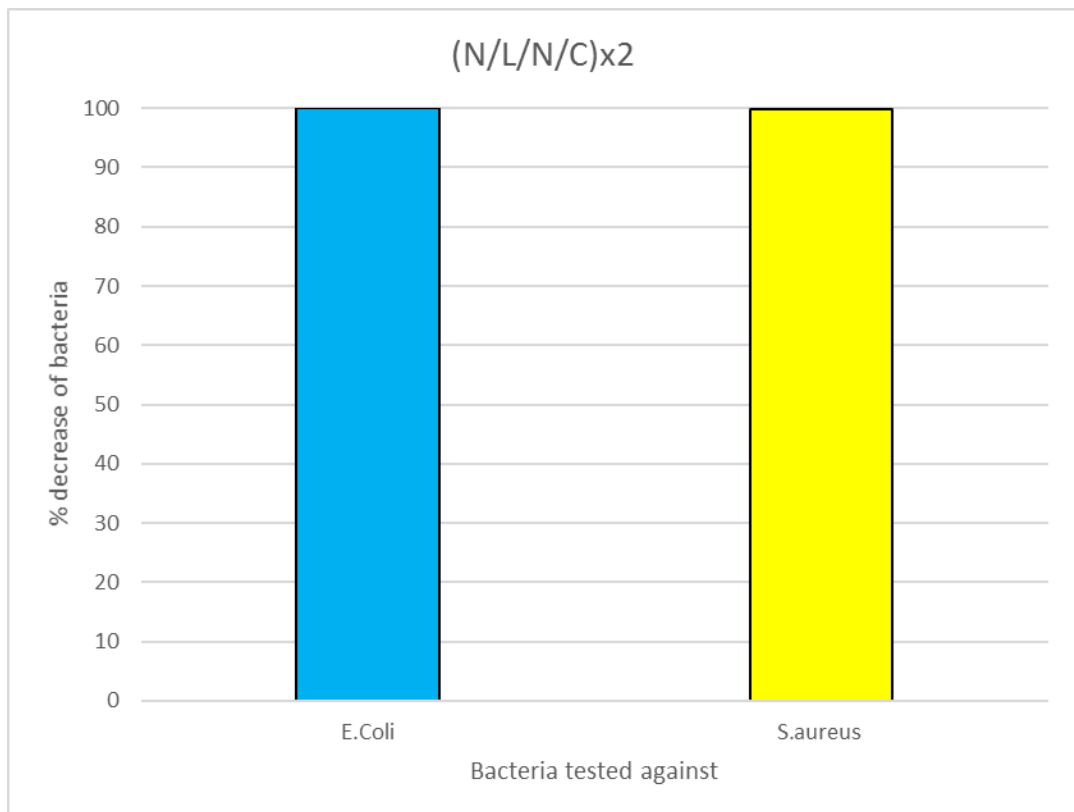


Figure 18. *Percentage decrease in E.coli and S.aureus bacteria incubated with (N/L/N/C)x2 coatings.*

Figure 18 it shows that the (N/L/N/C)x2 produced an average percentage decrease in bacteria of 99.95% for *E.coli* and 99.9% in *S.aureus*. In other words, (N/L/N/C)x2 coating shows an exceptionally high antimicrobial activity.

There have been many reports where lysozyme has been incorporated to layer-by-layer films for antimicrobial purposes. One report states how lysozyme was successfully deposited with gold nanoparticles in a layer-by-layer manner, resulting in significant antimicrobial performance<sup>2</sup>. Lysozyme, gold nanoparticles and tannic acid were assembled in an antimicrobial film<sup>44</sup>. Previous studies have shown chitosan to be used effectively for its antimicrobial properties within a layer-by-layer surface coating. One study reports chitosan/Pentasodium tripolyphosphate assemblies, that are able to inhibit *S.aureus*<sup>76</sup>. In another study, chitosan/ lentinan sulphate assemblies on a polyurethane surface showed advanced activity *P. aeruginosa*<sup>2</sup>.

#### 3.1.4 Atomic Force Microscopy (AFM) Analysis

AFM data in terms of 3-D and 2-D images for plates coated with Nafion, (N/L)x6, (N/C)x6 and (N/L/N/C)x2 are shown in Figures 19-22. AFM tests indicated a significant level of surface roughness for all coatings studies. As a general trend, a rough surface results in weaker bio-adhesion since the bacteria cannot get a firm grasp.

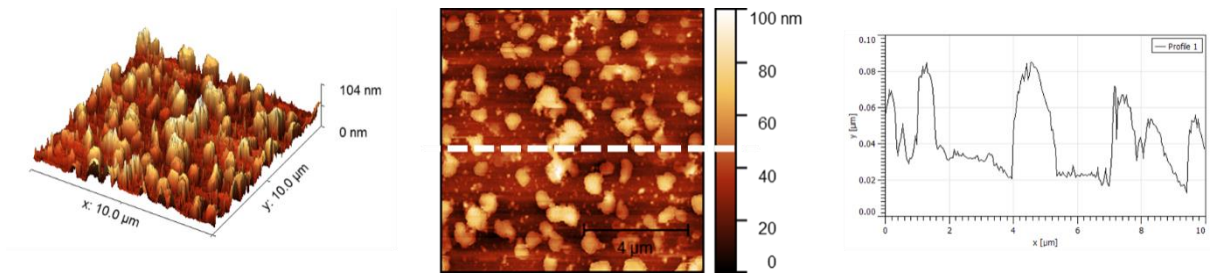


Figure 19. AFM of Nafion surface: 3-D image (left), 2-D image (middle), a graph showing the level of the surface roughness (right).

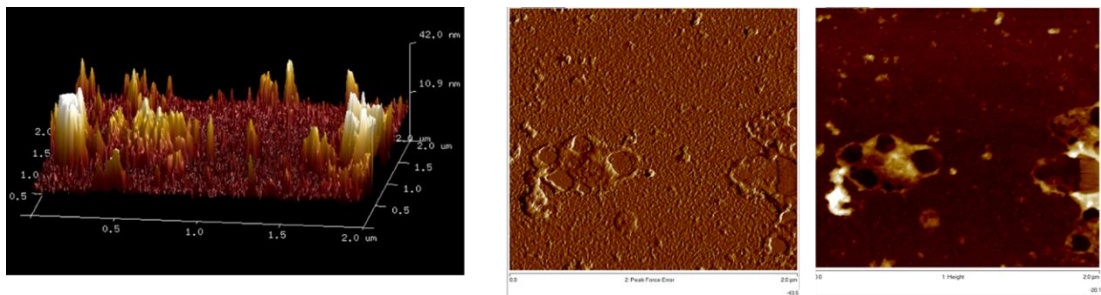


Figure 20. AFM of (N/L)x6 : 3-D image (left), 2-D images (middle and right).

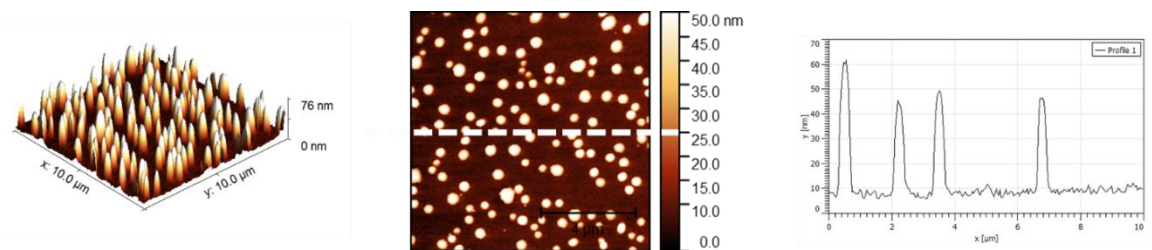


Figure 21. AFM of (N/C)x6 : 3-D image (left), 2-D image (middle), a graph showing the level of the surface roughness (right).

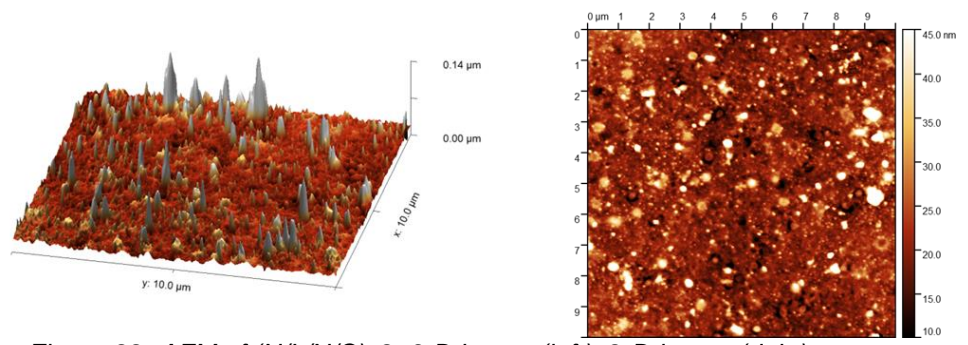
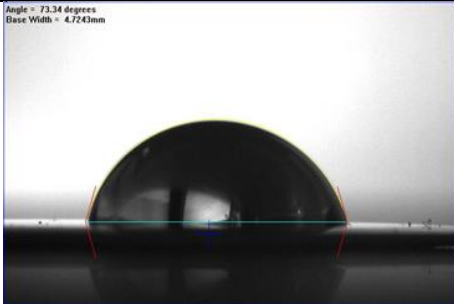
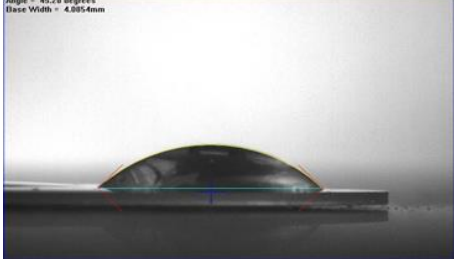
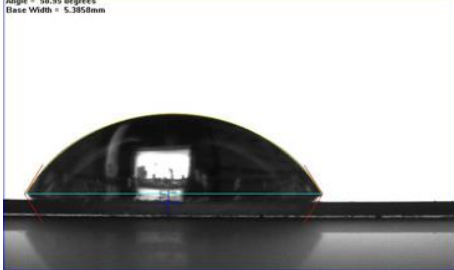
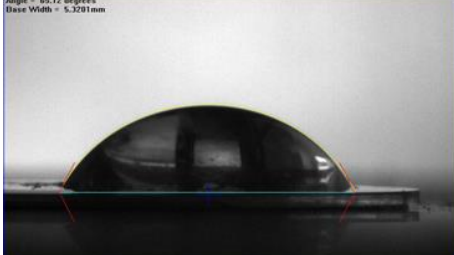


Figure 22. AFM of (N/L/N/C)x2: 3-D image (left), 2-D image (right).

### 3.1.5 Contact angles

Water contact angle tests were performed on the coatings and showed significant antimicrobial activity, with the results summarised in Table 1.

Table 1. *Water contact angle results for layer-by-layer deposits made from a combination of Nafion, lysozyme and chitosan.*

Multilayer systems	Average Contact angle (degrees)	Standard deviation	Picture
Nafion	72.94	0.65	 <p>Angle = 73.34 degrees Base Width = 4.7243mm</p>
(N/L)x6	45.29	0.014	 <p>Angle = 45.28 degrees Base Width = 4.8954mm</p>
(N/C)x6	58.92	1.186	 <p>Angle = 58.95 degrees Base Width = 5.3955mm</p>
(N/L/N/C)x2	64.08	1.77	 <p>Angle = 65.12 degrees Base Width = 5.3281mm</p>



The water contact angle of Nafion was found to be 73.3°. Nafion has been able to be shown as both hydrophobic and hydrophilic, when the contact angle was measured<sup>71</sup>. The measured contact angle for Nafion was 105°-110°, therefore showing Nafion to be hydrophobic. However, other tests the receding contact angle was shown to be 20° and 30° meaning that Nafion was showing a hydrophilic nature<sup>71</sup>. This gives the indication that Nafion surface is capable of switching between a hydrophobic and hydrophilic state. This is possible because the structure of Nafion has a cluster of sulfonic acid groups causing it to show hydrophilic behaviour. This is then surrounded by the backbone of tetrafluoroethylene (TFE), causing the Nafion to behave hydrophobically<sup>71</sup>. The contact angle for (N/L)x6 was found to be 45.3°, much lower than the contact angle that was observed for Nafion, showing that the surface is more readily wetted and more hydrophilic than the pure Nafion coating. The contact angle for (N/C)x6 was measured at 59.0°, showing the coating to be more hydrophobic than the (N/L)x6, but also more hydrophilic than the Nafion coating. The contact angle for (N/L/N/C)x2 was 65.1°, meaning that the coating was more hydrophobic than the other coatings, with the exception of the Nafion coating.

It is widely accepted that superhydrophobic coatings are more likely to show advanced antimicrobial activity, as they reduce the ability of the bacteria to adhere to the surface<sup>68</sup>. For example, hydrophobic silicon rubber exhibits superior antimicrobial properties in medical and household applications<sup>77</sup>. Another example is 3-(trimethoxysilyl)-propyldimethyloctadecyl ammonium chloride, which is a coating which has a hydrophobic surface with antimicrobial properties<sup>77</sup>. However, it has been reported that amphiphilic surfaces, where both hydrophobic and hydrophilic properties are shown, are also able to reduce

bacteria adhesion<sup>2</sup>. This has been shown where amphiphilic perfluoroalkyl polyethylene glycol was used in a layer-by-layer assembly and used to stop marine bacterium adhesion<sup>2</sup>.

### 3.1.6 UV-Vis analysis

The coatings (N/L/N/C)x2, (N/L)x6 and (N/C)x6 were also accessed with respect to their transparency properties, using UV-Vis spectroscopy as shown in Figure 23. Semi-micro polystyrene cuvettes were coated with the layer-by-layer systems, using dip layer method. This was achieved by dipping the surface of the cuvette in each of the materials being layered on, as well as being dipped in water between each layer to wash away any excess materials. The absorbance of light was measured for these against a non-coated cuvette, which acted as a control sample. The spectra was collected across a wavelength of 200 nm-900 nm.

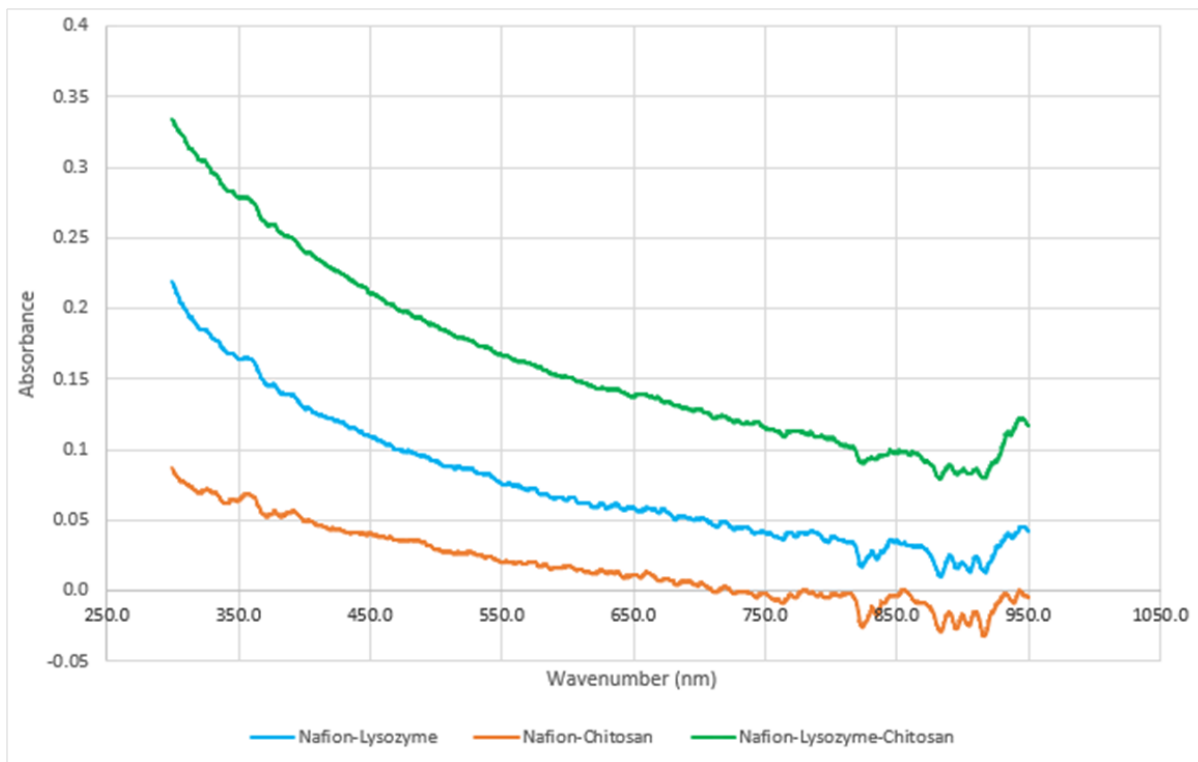


Figure 23. UV-Vis spectra for the layer-by-layer coatings for (N/L)x6 (blue points), (N/C)x6 (orange points) and (N/L/N/C)x2 (green points).

Figure 23 suggests that (N/L)x6 and (N/C)x6 showed lower absorbance than (N/L/N/C)x2. However, as shown in Figure 24, all coated cuvettes maintained their transparency. This means that the coatings can be used for application on surfaces that need to remain transparent, such as food packing and optical medical devices, but also possess antimicrobial properties to prevent the formation of bacteria.

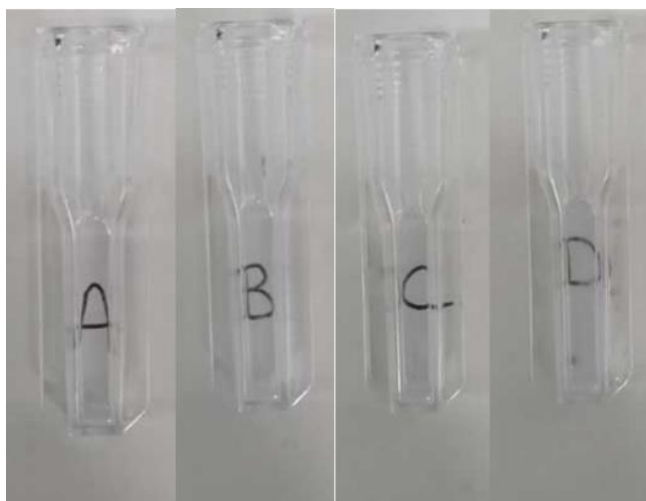


Figure 24. UV-vis cuvettes: uncoated (A), (N/L)x6 coated (B), (N/C)x6 coated (C), (N/L/N/C)x2 coated (D).

## 3.2 Nafion/QPDAEMA-PLMA assemblies

### 3.2.1 QCM-D

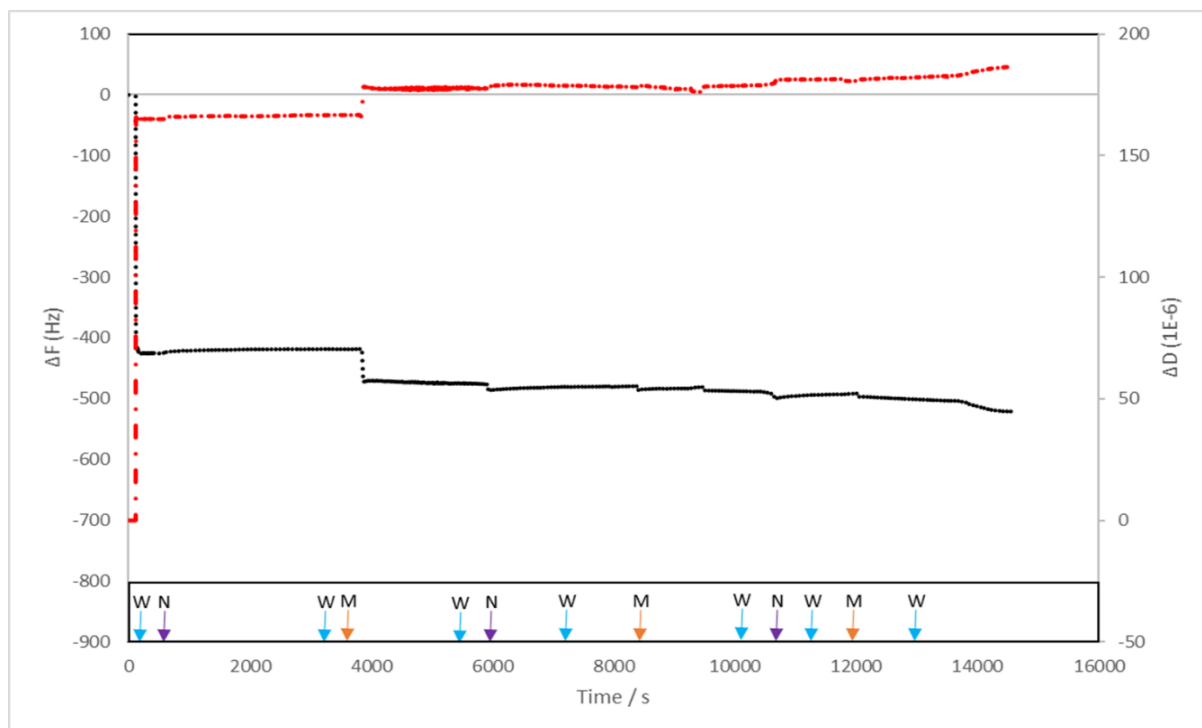


Figure 25. QCM-D sensograms for the layer-by-layer deposition of (N/M)x3. The letters W, N and M signify the addition of water, Nafion and QPDMAEMA-PLMA diblock, respectively.

Figure 25 shows the layer-by-layer deposition of (N/M)x4. The initial stages of this layering are the same as those in Figure 13, with the layering and interactions between the qater and the Nafion. The QPDMAEMA – PLMA Diblock is used as the positively charged layer.

### 3.2.2 Antimicrobial testing

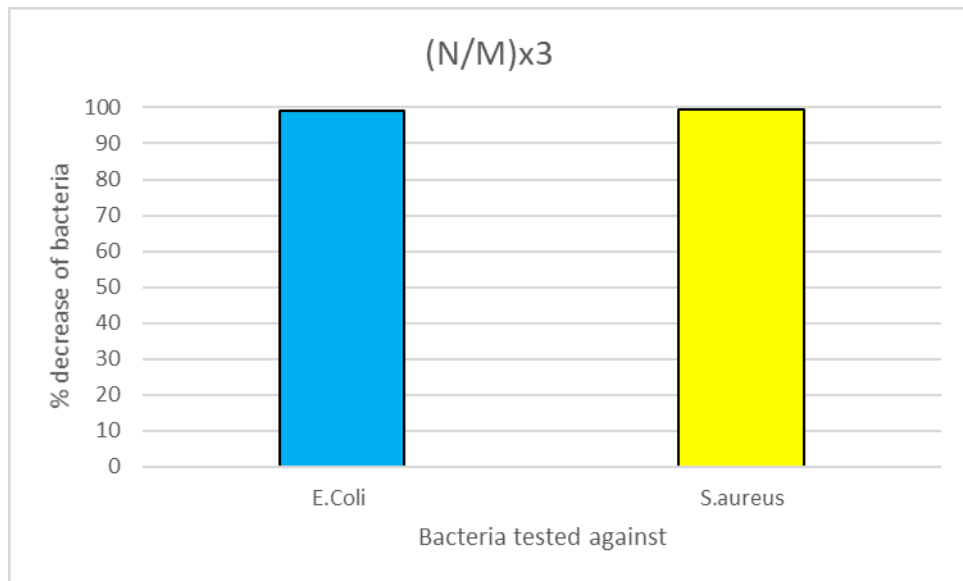


Figure 26. Percentage decrease in *E.coli* and *S.aureus* bacteria when tested against (N/M)x3 coatings.

Figure 26 shows (N/M)x3 giving an average percentage decrease of 99.155% against *E.coli* with an error of  $\pm 0.40305$  and 99.435% against *S.aureus* with an error of  $\pm 0.53033$ . This shows that (N/M)x3, has a significant antimicrobial effect against the bacteria, producing an average percentage decrease in bacteria above 99%, despite being not as effective against the bacteria as (N/L/N/C)x2..

### 3.3 Nafion/PVP assembly

#### 3.3.1 FT-IR

As with the previous FT-IR spectra, Figures 11 and 12, the Nafion and PVP combine mixture for FT-IR testing was made by mixing the Nafion and PVP together until precipitation occurred and then freeze drying it to form a solid sample that could be analysed on the FT-IR.

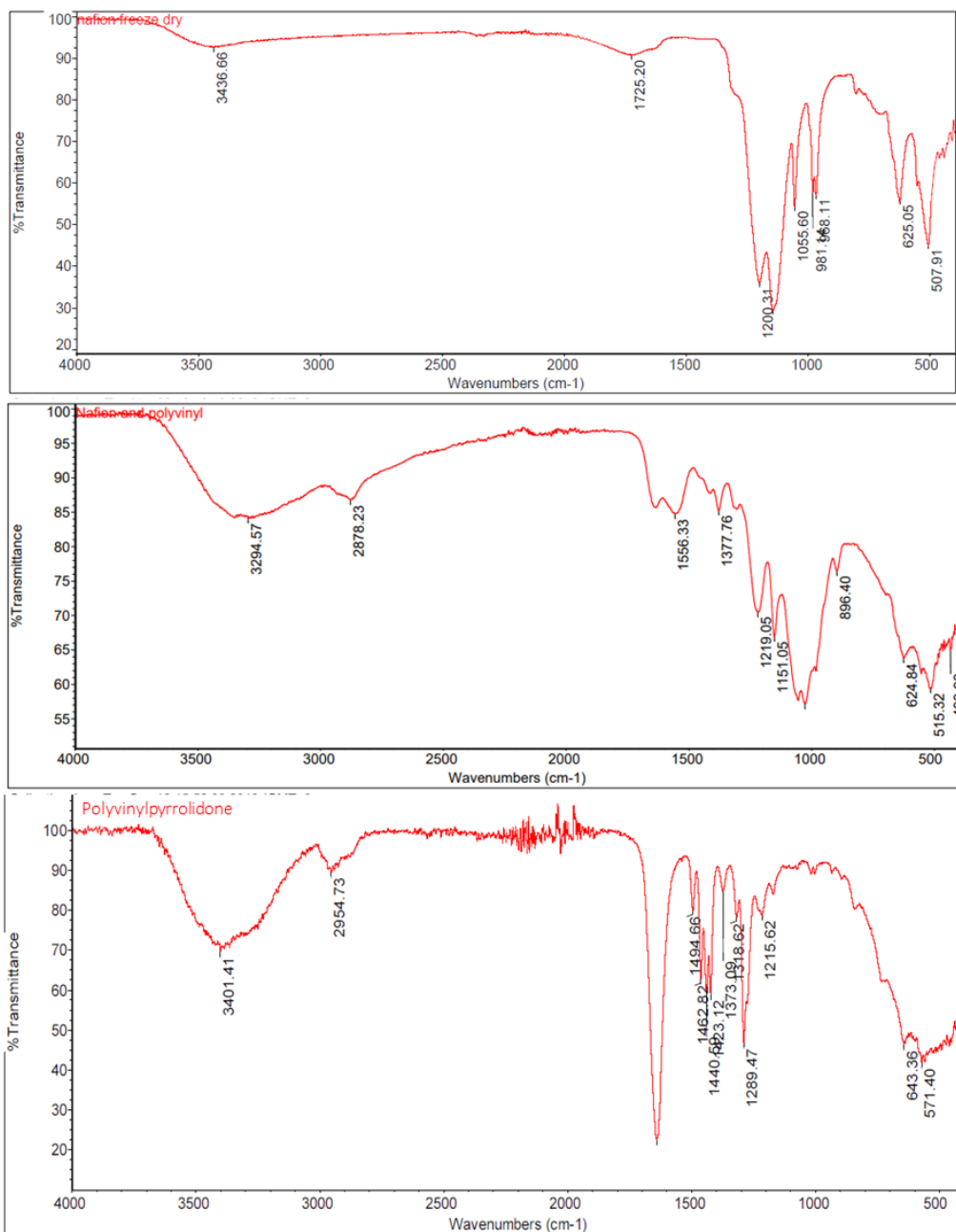


Figure 28. FT-IR spectra for Nafion (upper), Nafion/PVP blend (middle), and PVP (lower).

The FT-IR for Nafion shows peaks for the alkyl halide group C-F at  $1144\text{ cm}^{-1}$  and  $1055\text{ cm}^{-1}$ . In the Nafion-PVP blend, the peak for the C-F bond can still be seen at  $1151\text{ cm}^{-1}$  and  $1026\text{ cm}^{-1}$ . Nafion can also be identified in the Nafion spectrum by the C-O ether group, which is indicated by the peak at  $1200\text{ cm}^{-1}$ . In the spectrum for the blend of Nafion and PVP the peaks C-O ether bond can be



identified at  $1219\text{ cm}^{-1}$ . In the spectrum for PVP, carbonyl group  $\text{C}=\text{O}$ , which can be identified at  $1639\text{ cm}^{-1}$  and the N-H amide group can be seen by the peak at  $3401\text{ cm}^{-1}$ . The N-H amide group in PVP can still be identified in the Nafion/PVP bend spectra but at  $3294\text{ cm}^{-1}$ . The spectrum for the blended Nafion and PVP shows shifts in the N-H and  $\text{C}=\text{O}$  groups in comparison with the other two spectrums. This can be explained by possible hydrogen bonding effect taking place between the two molecules when they combine together. Hydrogen bonding effects happen when the hydrogen bonding between the two molecules cause the modes to vibrate at lower frequencies and broaden<sup>78</sup>.

### 3.3.2 QCM-D

The initial layering of (N/P)x3 is by the same interactions as in the previous QCM-D data, with Water and Nafion interacting through the same electrostatic interactions, as described in the previous QCM-D graphs in Figure 13. The positively charged layer is made up of PVP. This is positively charged and interacts with the Nafion through electrostatic interactions. As seen in Figure 29.

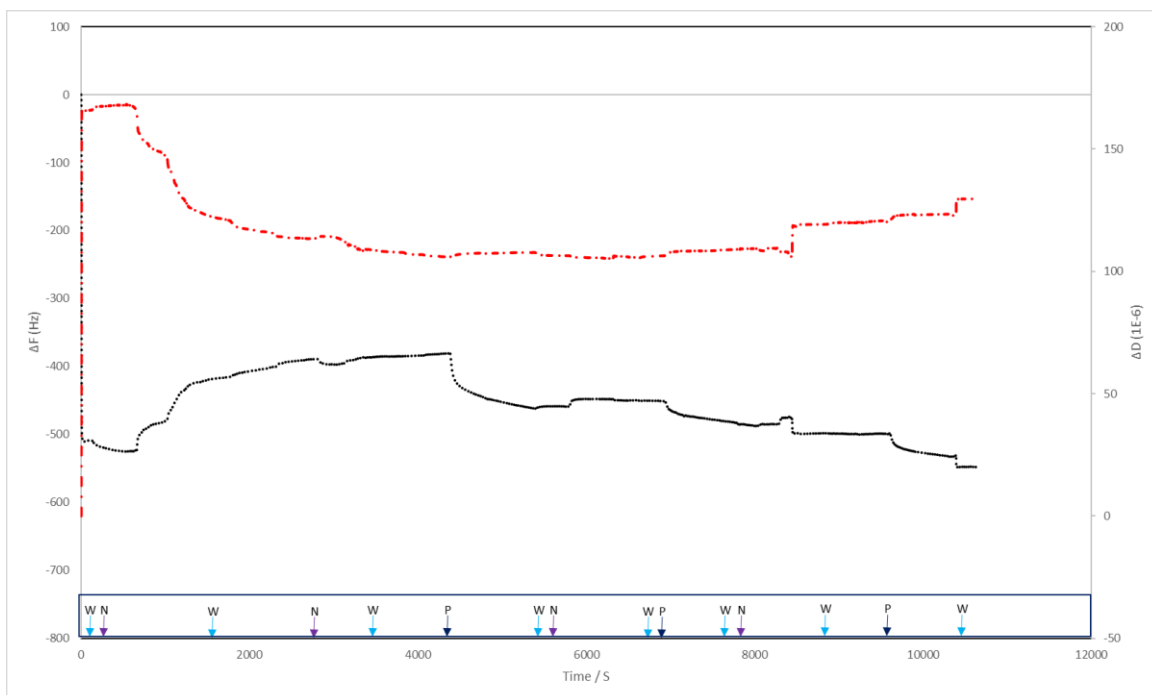


Figure 29. QCM-D sensogram for the layer-by-layer deposition of (N/P) $\times$ 3. The letters W,N,P denote the introduction of water, Nafion and PVP, respectively.

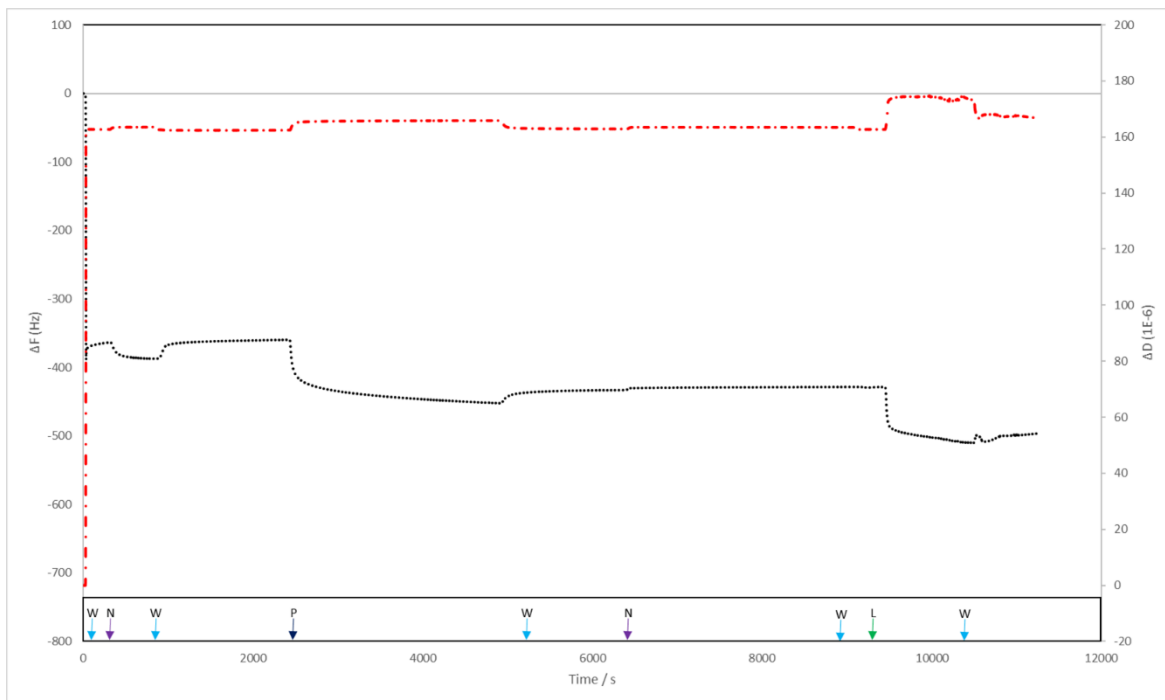


Figure 30. Layer-by-layer deposition of (N/P/N/L) $\times$ 1. The letters W, N, P, L denote the injection of water, Nafion, PVP and lysozyme, respectively.

Figure 30 shows the layer-by-layer deposition for (N/P/N/L) $\times$ 1. This has the same layering and electrostatic interactions between the water and Nafion as previously stated. The positive layers were made up of PVP and lysozyme, which were alternatively added on.

### 3.3.3 Antimicrobial testing

Figure 31 shows the average percentage decrease of (N/P)x3, when tested against *E.coli* was 74%. The average percentage decrease for *S.aureus* was more significant with the (N/P)x3 coating showing a 92% bacteria decrease.

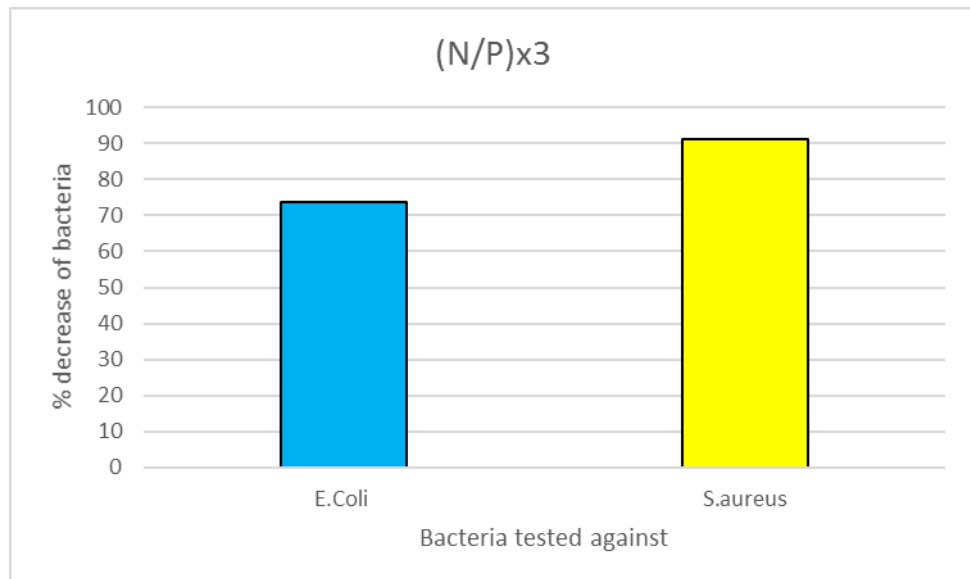


Figure 31. Percentage decrease in *E.coli* and *S. aureus* incubated with (N/P)x3 coating

Incubation with (N/P/N/C)x1 results in 99.6% *E.coli* reduction and 96.5% *S.aureus* suppression as seen in Figure 32.

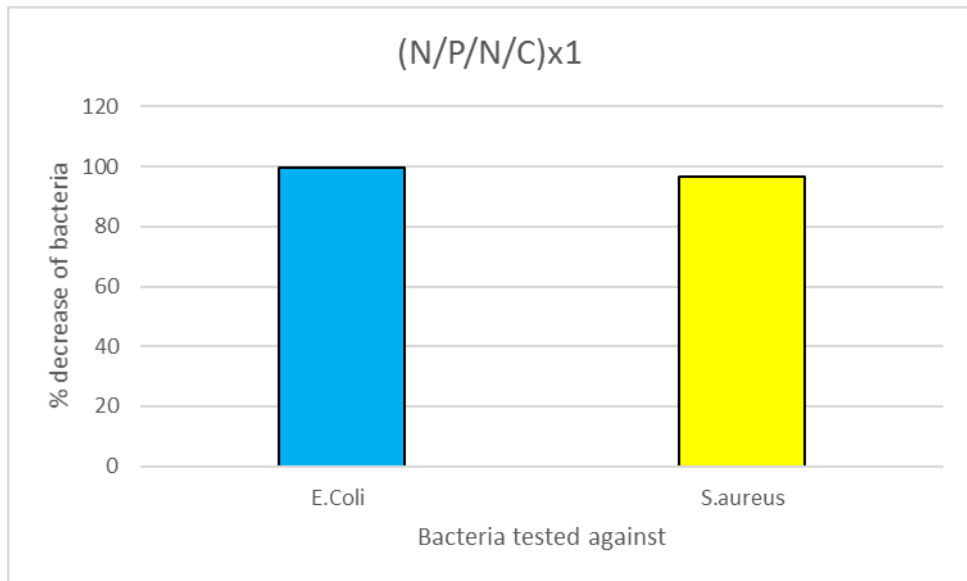


Figure 32. Percentage decrease in *E.coli* and *S.aureus* bacteria incubated with (N/P/N/C)x1 coating.

Figure 33 shows that incubation with (N/P/N/L)x1 results in more than 99% *S.aureus* reduction, compared to only 60 % *E.coli* suppression.

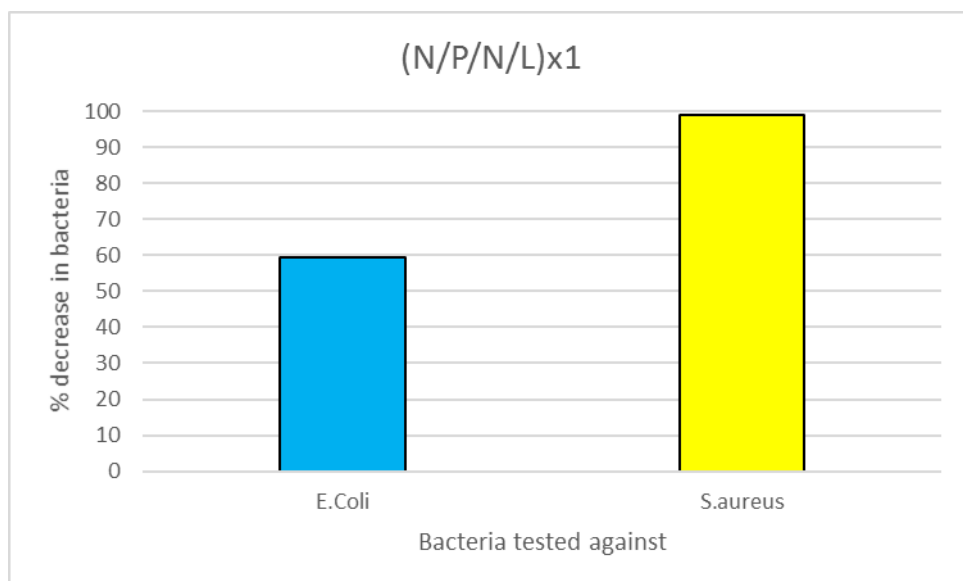
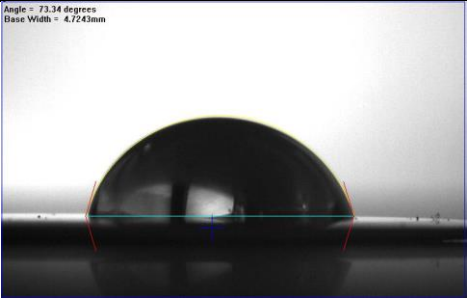
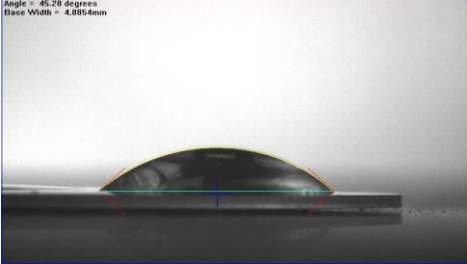

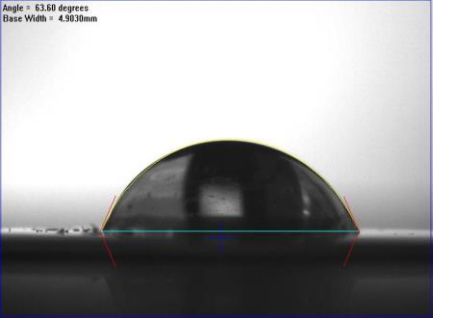


Figure 33. Percentage decrease in *E.coli* and *S.aureus* bacteria incubated with (N/P/N/L)x1 coating.

### 3.3.4 Contact angles

As seen in Table 2, introduction of lysozyme to the assembly reduces the contact angle from 73.3° to 45.3°, while further incorporation of PVP partially restores the value to 63.6°. While superhydrophilic and superhydrophobic materials are typically desired for antimicrobial purposes, surfaces with intermediate contact angles might also show superior biocide properties<sup>79</sup>.

Table 2. Water contact angles for surfaces coated with various Nafion based layer by layer assemblies.

Multilayer system	Average Contact angle (degrees)	Standard deviation	Picture
Nafion	72.94	0.65	 <p>Angle = 73.34 degrees Base Width = 4.1243mm</p>
(N/L)x6	45.29	0.014	 <p>Angle = 45.28 degrees Base Width = 4.0954mm</p>
(N/P)x3	75.1	0	 <p>Angle = 75.12 degrees Base Width = 4.2141mm</p>
(N/P/N/L)x1	62.71	1.53	 <p>Angle = 63.60 degrees Base Width = 4.3030mm</p>

# Chapter Four

## Summary and Conclusion

### 4.1 Summary

The study focuses on a new generation of layer by layer assemblies with superior antimicrobial properties. Nafion was employed as the negatively charged polymer, while lysozyme, chitosan, PVP were used as the positively charged building blocks. FT-IR spectra suggests the presence of attractive forces between the alternating layers, an effect that gives rise to durable and robust coatings.

The QCM-D was used to monitor *in situ* the construction of (N/L)x6, (N/C)x6, (N/L/N/C)x2, (N/M)x3, (N/P)x3, (N/P/N/C)x1 and (N/P/N/L)x1. In most cases, the steep decrease in oscillating frequency after each deposition step, indicated significant adsorption of the alternating layers. All coatings showed advanced antimicrobial performance against model gram-positive and gram-negative strains. Among the various systems, (N/L/N/C)x2 and (N/L)x6 were found to suppress the growth of both *E.coli* and *S.aureus* by more than 99.9%.

AFM analysis was used to examine the surface topology of (N/L)x6, (N/C)x6 and (N/L/N/C)x2 and a coating of Nafion . All coatings show high levels of surface roughness and water wettability values within the range 75-45°. Significantly, all coatings retain their transparent nature, a highly desirable effect for application relate to food packaging and optical devices. Given that this type of coatings combines a number of unique characteristics, they show great potential for a wide range of antimicrobial applications.

## 4.2 Conclusion

This study demonstrates that Nafion-based materials give rise to layer-by-layer coatings, which contain supreme structural stability and durability, which relies on electrostatic forces between oppositely charged molecules and particle-particle H-bonding. The exceptional antimicrobial properties of the coatings reflect the action of 3 different parameters: the contact kill behaviour of components (lysozyme, chitosan, QPDMAEMA-PLMA diblock copolymer and PVP), the bacterial repellent behaviour of Nafion and the surface topology of the coatings. In that sense the study paves the way for the development of a new generation of highly effective materials with advanced efficiency against pathogens.



# References

1. Founou R, C., Founou LL, Essack SY. Clinical and economic impact of antibiotic resistance in developing countries: A systematic review and meta-analysis. *PLOS ONE*. 2017;12(12):e0189621.
2. Zhu X, Loh X, Jun. Layer-by-layer assemblies for antibacterial applications. - *Biomater Sci*. 2015(12):1499-1580.
3. Muhsin J, Wisal A, Saadia A, et al. Bacteria biofilm and associated infections. *Journal of the Chinese Medical Association*. 2018;81(1):7-11.
4. Grossman R, F., Nwabunma D. *Functional polymer coatings. principles, methods, and applications*. John Wiley and Sons; 2015.
5. Stephens C. Microbiology: Breaking down biofilms. *Current Biology*. 2002;12(4):132-134.
6. Ventola C, Lee. The antibiotic resistance crisis. *Pharmacy and Therapeutics*. 2015;4(40):277-283.
7. Swartjes J, Sharma PK, van Kooten T, G., et al. Current developments in antimicrobial surface coatings for biomedical applications. *Current Medical Chemistry*. 2015;22(18):2116-2129.
8. Veiga S, Ana., Schnider J, P. Antimicrobial hydrogels for the treatment of infection. *Biopolymers*. 2013;100(6):637-644.

9. Wang G, Mirshra B. Mechanism of action of tethered antimicrobial peptides. In: Tiwari A, ed. *Handbook of antimicrobial coatings*. 1st ed. Elsevier Inc.; 2018:559-566.
10. Dong A, Wang Y, Gao Y, Gao G. Chemical insights into antibacterial N-halamines. *Chemical Review*. 2017;6(117):4806-4862.
11. Cerkez I. N-halamine-based antimicrobial coatings. In: Tiwari A, ed. *Handbook of antimicrobial coatings*. 1st ed. Elsevier Inc.; 2018:391-409.
12. Wang Y, Tong SW, Xu XF, Özyilmaz B, Loh KP. Interface engineering of layer-by-layer stacked graphene anodes for high-performance organic solar cells. *Adv Mater*. 2011;23(13):1514-1518.
13. Ariga K, Lvov Y, Kawakami K, Ji Q, Hill J. Layer-by-layer self-assembled shells for drug delivery. *Advanced drug delivery reviews*. 2011:762-771.
14. Decher G, Eckerle M, Schmitt J, Struth B. Layer-by-layer assembled multicomposite films. *Current Opinion in Colloid & Interface Science*. 1998;3(1):32-39.
15. Picart C, Carusco F, Voegel J. Subcompartmentalized surface-adhering polymer thin film towards drug delivery applications. In: *Layer-by-layer films for biomedical applications*. Wiley; 2014:207-208.
16. Michel M, Izquiere A, Decher G, Voegel J, Schaaf P, Ball V. Layer by layer self-assembled polyelectrolyte multilayers with embedded phospholipid vesicles obtained by spraying: Integrity of the vesicles. *Langmuir*. 2005;21(17):7854-7855.

17. Bachner M, Poh Y, Serbowicz T, Vozar S. The spin-grower: A machine for rapid layer-by-layer assembly of nanostructured materials. . 2008:1-81.
18. Nogueira G, M., Banerjee D, Cohen R, E., Rubner Michael F. Spray-layer-by-layer assembly can more rapidly produce optical-quality multistack heterostructures. *Langmuir*. 2011;27(12):7860-7866.
19. Jiang C, Markutsya S, Tsukruk V, V. Collective and individual plasmon resonances in nanoparticle films obtained by spin-assisted layer-by-layer assembly. *Langmuir : the ACS journal of surfaces and colloids*. 2004;20(3):882-890.
20. Cho J, Char K, Hong J-, Lee K-. Fabrication of highly ordered multilayer films using a spin self-assembly method. *Adv Mater*. 2001;13(14):1076-1078.
21. Jampilek J, Kralova K. Nanoantimicrobials: Activity, benefits and weaknesses. In: Fikai A, Grumezesu A, eds. *Nanostructures for antimicrobial therapy*. 1st ed. Elsevier Inc.; 2017:23-42.
22. Singh A, K. Structure, synthesis and applications of nanoparticles. In: *Engineered nanoparticles. structure, properties and mechanisms f toxicity*. Elsevier Inc.; 2016:19-76.
23. Massa M, A., Covarrubias C, Bittner M, et al. Synthesis of ner antibacterial composite coating for titanium based on highly ordered nanoporous silica and silver nanoparticles. *Materials Science and Engineering C*. 2014;45:146-153.
24. Zhang X, Liu Z, Shen W, Gurunathan S. Silver nanoparticles: Synthesis, characterization, properties, applications, and therapeutic approaches. *International Journal of Molecular Sciences*. 2016;17(9):1-34.

25. Kim J, Sung., Kuk E, Yu K, Nam., et al. Antimicrobial effects of silver nanoparticles. *Nanomedicine: Nanotechnology, Biology and medicine*. 2007;3(1):95-101.
26. Elbourne A, Crawford R, Ivanova E, P. Nano-structured antimicrobial surfaces: From nature to synthetic analogues. *Journal of Colloid and Interface Science*. 2017;508:1-616.
27. Wang L, Hu C, Shao L. The antimicrobial activity of nanoparticles: Present situation and prospects for the future. *International Journal of Nanomedicine*. 2017;12:1227-1249.
28. Zhang X, Liu Z, Shen W, Gurunathan S. Silver nanoparticles; sythesis, characterization, properties, applications, and therapeutic approaches. *International Journal of Molecular Sciences*. 2016;17(9):1534-1567.
29. El-Nour, Kholoud, M, M, Abou., Eftaiha A, Al-Warthan A, Ammar, Reda, A, A. Synthesis and applications of silver nanoparticles. *Arabian*. 2010;3(3):135-140.
30. Ramyadevi J, Jeyasubramanian K, Marikani A, Rajakumar G, Rahuman A, Abdul. Synthesis and antimicrobial activity of copper nanoparticles. 2012. *Materials Letter*;71:114-116.
31. Dubas ST, Kumlangdudsana P, Potiyaraj P. Layer-by-layer deposition of antimicrobial silver nanoparticles on textile fibers. *Colloids and Surfaces A: Physicochemical and Engineering Aspects*. 2006;289(1):105-109.
32. Gomes AP, Mano JF, Queiroz JA, Gouveia IC. Layer-by-layer deposition of antimicrobial polymers on cellulosic fibers: A new strategy to develop bioactive textiles. *Polym Adv Technol*. 2013;24(11):1005-1010.

33. Crekez I, Kocer H, Worley S, Broughton R, Huang T. N-halamine biocidal coatings via a layer-by-layer assembly technique. - *Langmuir*. 2011(7):4091-4097.
34. Huang K, Yang C, Huang S, Chen C, Lu Y, Lin Y. Recent advances in antimicrobail polymers: A mini review. *International Journal of Molecular Sciences*. 2016;17(9):1-14.
35. Bastarrachea L, J., Goddard J, M. Self-healing antimicorbial polymer coating with efficacy in the presence of organic matter. *Applied Surface Science*. 2016;378:479-488.
36. Hung Y, McLandsbourough L, A., Goddard J, M., Bastarrachea L, J. Antimicrobial polymer coatings with effiacy against pathogenic and spoilage microorganisms. *LWT*. 2018;97:546-554.
37. Plascoat. Durable, abrasion and micrbial resistant plastic coatings for medical furniture. <http://www.plascoat.com/en-gb/coating-applications/medical-furniture.html>. Accessed October, 2017.
38. Plascoatt The Art of protection. Maldon shotblasting and powderr coating. <http://www.ctc-powder-coating.co.uk/our-work/plascoat/>. Updated 2016. Accessed October, 2017.
39. AIC Coatings. Rilsan nylon coating applications. <http://www.aic-coatings.com/>. Updated 2013. Accessed October, 2017.
40. Kariduraganavar M Y, Kittur A, A., Kamble R, R. Polymer synthesis and processing. In: Kumbar S, G., Laurencin C, T., Deng M, eds. *Natural and sythestic biomedical polymers*. Elsevier; 2014:1-31.

41. Goy R,C., Morais, S,T,B., Assis, O,B,G. Evaluation of the antimicrobial activity of chitosan and its quaternized derivative on E.coli and S. aureua growth. *Brazilian Journal of Pharmacognosy*. 2016;26(1):122-127.
42. Goy R,C., De Britto D, Assis, O,B,G. A review of the antimicrobial activity of chitosan. . 2009;19(3):241-247.
43. Mahmoudi N, Ostadhossien F, Simchi A. Physicochemical and antibacterial properties of chitosan-polyvinylpyrrolidone films containing self oraganized graphene oxide nanolayers. *Journal of Applied Polymer Science*. 2015;133(11):1-8.
44. Zhou B, Jin X, Li J, et al. Vacuum-assisted layer-by-layer electrospun membranes: Antibacterial and antioxidative applications. . 2014;4:54517-54524.
45. Primo E, Otero L, Ruiz F, Klinke S, Giordano W. - The disruptive effect of lysozyme on the bacterial cell wall explored by an in-silico structural outlook: Effect of lysozyme on the bacterial cell wall. - *Biochemistry and Molecular Biology Education*. 2017:-.
46. Ibrahim H, R., Kato A, Kobayashi K. Antimicrobial effects of lysozyme against gram-negative bacteria due to covalent binding of palmitic acid. - *J Agric Food Chem*. 1991;39(11):2077.
47. Sigma-Aldrich. Lysozyme from chicken egg white. <https://www.sigmaaldrich.com/catalog/product/sigma/l6876?lang=en&region=G>  
B. Updated 20182018.

48. Prakash S, Mustain E, W., Khol P, A. Electrolytes for long-life, ultra low-power direct methanol fuel cells. In: Zhao T, S., ed. *Micro fuel cells*. Elsevier Inc.; 2009:1-50.
49. Leddy J. Modification of nafion membranes: Tailoring properties for function. In: Liu J, L., Bashir S, eds. *Nanomaterial for sustainable energy*. American Chemical Society; 2015:99-133.
50. Lefaux CJ, Kim B, Venkat N, Mather PT. Molecular composite coatings on nafion using layer-by-layer self-assembly. - *ACS Appl Mater Interfaces*. 2015;7(19):10365-10373.
51. Zhong L, J., Pang L, Q., Che L, M., Wu X, E., Chen X, D. Nafion coated stainless steel for anti-biofilm application. *Colloids and Surfaces B: Biointerfaces*. 2013;111:252-256.
52. Abd El-Mohdy HL, Ghanem S, J. Biodegradability, antimicrobial activity and properties of PVA/PVP hydrogels prepared by  $\gamma$ -irradiation. - *Journal of Polymer Research*. 2009;16(1):1-10.
53. Soshee A, Zurcher S, Spencer N, D., Halperin A, Nizak C. General in vitro to analyze the interactions of synthetic polymers with human antibody repertoires. *Biomacromolecules*. 2014;15(1):113-121.
54. Louie S, M., Gorham J, M., Tan J, Hackley VA. Ultraviolet photo-oxidation of polyvinylpyrrolidone (PVP) coatings on gold nanoparticles. - *Environ Sci : Nano*. 2017;4(9):1866-1875.
55. Silhavy T, J., Kahne D, Walker S. The bacterial cell envelope. *Cold Spring Harbor Laboratory Press*. 2014.

56. Wirtanen G, Salo S. Biofilm risks. In: Lelieveld H, Holah J, Garric D, eds. *Handbook of hygiene control in the food industry*. 2nd ed. Elsevier Ltd.; 2016:55-79.
57. Percival S, L., Williams D, W. Escherichia coli. In: Percival S, L., Yates M, V., Gray N, F., eds. *Microbiology of waterborne disease*. 2nd ed. Elsevier Ltd.; 2014:89-117.
58. Liu D. Escherichia coli. *Reference Modules in Biomedical Sciences*. 2014:125-132.
59. Ossila. Spin coating: A guide to theory and techniques. <https://www.ossila.com/pages/spin-coating#spin-coating-general-theory>. Updated 20182018.
60. Dixon M, C. Quartz crystal microbalance with dissipation monitoring: Enabling real-time characterization of biological materials and their interactions. *Journal of Biomolecular Techniques : JBT*. 2008;19(3):151-158.
61. Peak D. Fourier transform infrared spectroscopy. *Encyclopedia of soils in the environment*. 2005:80-85.
62. Last J,A., Russell P, Nealey P, F., Murphy C, J. The applications of atomic force microscopy to vision science. . 2010;51(12).
63. Orbay S, E., Alaskari A, M. Atomic force microscopy (AFM) topographical surface characterization of multilayer-coated and uncoated carbide inserts. *World Academy of Science, Engineering and Technology*. 2010;4(10):977-988.



64. Yuan Y, Randall Lee T. Contact angle and wetting properties. In: Bracco G, Holst B, eds. *Surface science techniques*. Springer-Verlag Berlin Heidelberg; 2013:3-34.
65. Hebbar R, S., Isloor A,M., Ismail A, F. Contact angle measurements. In: Hilal N, Ismail A, F., Matsuura T, Oatley-Radcliffe D, eds. *Membrane characterization*. Elsevier; 2017:219-255.
66. Fritsch A, Willmott G, Taylor M. Superhydrophobic new zeland leaves: Contact angle and drop impact experiments. *Journal of the Royal Society of Zealand*. 2013;43(4):198-210.
67. Chau T, T., Bruckard W, j., Koh, P, T, L., Nguyen A, V. A review of the factors that affect contact angle and implications for the flotation practice. *Advances in Colloid and Interface Science*. 2009;150(2):106-115.
68. Aslanidou D, Karapanagiotis I. Superhydrophobic, superoleophobic and antimicrobial coatings for the protection of silk textiles. *Coatings*. 2018;8(3):1-13.
69. Salman S, R. Electronic spectroscopy, study of chemical reactions. In: *Encyclopedia of spectroscopy and spectrometry*. 3rd ed. Elsevier; 2017:470-475.
70. Worsfold PJ, Zagatto EAG. Spectrophotometry:Overview. In: Worsfold P, Townshend A, Poole C, eds. *Encyclopedia of analytical science*. 2nd Edition ed. Oxford: Elsevier; 2005:218-321.
71. Goswami S, Klaus S, Benziger J. Wetting and absorption of water drops on nafion films. *Langmuir*. 2008;24(16):8627-8633.

72. Fernandes D, Kluska W, Stanislawska J, Board B, Krysmann M, J., Kellarakis A. Novel hydrogels containing nafion and poly(ethylene oxide) based block copolymers. *Polymer*. 2017;114:73-78.
73. Kellarakis A, Giannelis E, P. Nafion as consurfactant: Solubilization of nafion in water in the presence of pluronics. *Langmuir*. 2010;27(2):554-560.
74. Kellarakis A, Krysmann M, J. Trivial and non-trivial superamolecular assemblies based on nafion. *Colloids and Interface Science Communications*. 2014;1:31-41.
75. Zhou B, Li Y, Deng H, Hu Y, Li B. Antibacterial multilayer films fabricated by layer-by-layer immobilizing lysozyme and gold nanopartilces on nanofibers. *Colloids and Surfaces B: Biointerfaces*. 2014;116:432-438.
76. Shirvan A, Rouhani., Nejad N, Hemmati., Bashari A. Antibacterial finishing of cotton fabric via the chitosan/TPP self-assembled nano layers. *Fibers and Polymers*. 2014;15(9):1908-1914.
77. Rauner N, Mueller C, Ring S, et al. A coating that combines lotus-effect and contact-active antimicrobial properties on silicone. *Advanced functional materials*. 2018;28(29):1-9.
78. Fornaro T, Burini D, Biczysko M, Barone V. Hydrogen-bonding effects on infrared spectra from anharmonic computations: Uracil-water complexed and uracil dimers. *The Journal of physical chemistry A*. 2015;119(18):4224-4236.
79. Zhu X, Janczewski D, Guo S, et al. Polyion multilayers with precise surface charge control for antifouling. *Applied materials and interfaces*. 2015;7(1):852-861.

